THE SEISMIC STRATIGRAPHY AND SEDIMENTATION ALONG THE NINETYEAST RIDGE

A Thesis

by

AMY ELIZABETH EISIN

Submitted to the Office of Graduate Studies of
Texas A&M University
in partial fulfillment of the requirements for the degree of

MASTER OF SCIENCE

August 2009

Major Subject: Oceanography

THE SEISMIC STRATIGRAPHY AND SEDIMENTATION

ALONG THE NINETYEAST RIDGE

A Thesis

by

AMY ELIZABETH EISIN

Submitted to the Office of Graduate Studies of
Texas A&M University
in partial fulfillment of the requirements for the degree of

MASTER OF SCIENCE

Approved by:

Chair of Committee, William Sager
Committee Members, Richard Gibson
Mitch Lyle
Head of Department, Piers Chapman

August 2009

Major Subject: Oceanography

ABSTRACT

The Seismic Stratigraphy and Sedimentation along the Ninetyeast Ridge.

(August 2009)

Amy Elizabeth Eisin, B.S., University of Illinois at Urbana-Champaign

Chair of Advisory Committee: Dr. William Sager

The Ninetyeast Ridge (NER) is a ~5000 km-long aseismic volcanic ridge trending N-S in the eastern Indian Ocean basin. It is widely accepted that NER formed from the trace of a single hotspot as the Indian plate moved northward during the Late Cretaceous and Early Cenozoic due to the linear age progression from 43 Myo at the southern end to 77 Myo at the northern end. What is not fully understood is the geologic history of the ridge since its formation. This study examines the stratigraphy and sediment thickness on the ridge using new seismic data to describe the sedimentary history of NER.

More than 3700 km of 2D multichannel seismic reflection profiles were collected along NER at seven sites between 5.5° N and 26.1° S during cruise KNOX06RR of the R/V *Roger Revelle* in 2007. Scientific objectives were to obtain site survey data for proposed drilling and to understand the sedimentary layers, sediment distribution, and geologic history of NER. Seismic survey sites were chosen primarily based on proximity to existing Deep Sea Drilling Project (DSDP) and Ocean Drilling Program (ODP) drill holes (Sites 758, 216, 214, and 253) for interpretation and correlation with existing lithologic data.

Seismic data were processed (filtered, stacked, and time-migrated) and interpreted using standard seismic stratigraphy principles. Three major horizons were interpreted,

correlated with those previously recognized at the DSDP and ODP sites, and traced throughout the seismic data. Seismic data were categorized into three units based on distinct acoustic properties including changes in reflector amplitude, wavelength, continuity, and geometry. Seismic Unit I comprises a succession of pelagic sediments and sedimentary rock draped over Seismic Unit II, which consists of pelagic carbonates mixed with volcaniclastics. Seismic Unit III is volcanic basement.

Sediment layer thicknesses and distribution were mapped at each site, and bathymetric data were correlated with seismic data to interpret geologic features. Seismic and core data indicate a common sedimentary history at each site: volcaniclastic-rich sediments deposited during or shortly after ridge formation topped by a thick drape of pelagic sediments. This history likely happened in three stages over the last ~77 My: 1) the initial subaerial or submarine emplacement of the volcanic ridge, 2) the deposition of shallow water sediments and volcaniclastics, and finally 3) the subsidence of the ridge followed by deep water pelagic sediment deposition.

NOMENCLATURE

DSDP	Deep Sea Drilling Project
IODP	Integrated Ocean Drilling Program
KNOX06RR	Scripps Institution of Oceanography cruise designation
MBSF	Meters (m) below seafloor
Myo	Million years old
NER	Ninetyeast Ridge
ODP	Ocean Drilling Program
QC	Quality Checked
SEG-Y	Society of Exploration Geophysicists, “Y” file format
SMT KINGDOM	Seismic Micro Technology Kingdom Suite software package
TWTT	Two-way travel time, in seconds (s)

A *seismic reflector* marks a boundary between beds with different physical properties, including changes in lithology, which cause sound waves to be reflected and can comprise either a single peak or trough or a sequence of them.

A *horizon* is a line drawn across the seismic profile, either electronically or on paper, as an interpretation of either individual beds, or succession of beds that represent a related unit of seismic reflectors sharing distinct acoustic properties. The ability to distinguish individual beds will, of course, depend on the degree of seismic resolution.

Acoustic basement is the portion of the Earth below which strata cannot be imaged with seismic data, or the deepest relatively continuous reflector or series of reflectors. In some regions it coincides with geologic basement, or that portion of the Earth that does not comprise sedimentary rocks. Often times, the acoustic basement *reflector* marks an obvious change in acoustic properties (usually strong impedance contrast) or change from coherent to chaotic reflectors (modified from Gillis, 2009).

TABLE OF CONTENTS

LIST OF FIGURES

LIST OF TABLES

CHAPTER I

INTRODUCTION

This study uses the seismic data acquired on cruise KNOX06RR aboard the R/V *Roger Revelle*, a 2007 site survey cruise for proposed drilling (IODP Drilling Proposal #620). The cruise purpose was to better understand the stratigraphy, sediment thickness and distribution, and geologic history of the Ninetyeast Ridge (NER). Because these data show details of sediment layers, the basement surface, and faulting, they can be used to select drill sites and to help understand the origin and evolution of the NER, and to determine whether the single hotspot model is the best explanation for its formation (Sager et al., 2007).

Most of the seismic data that exist for the NER are sparse, old, and of poor quality. Although many research cruises have crossed the NER and vicinity to collect geophysical data including seismic reflection profiles, most of them have been in the form of a single traverse across the ridge to collect single channel, analog seismic data, and were not GPS navigated. The seismic data collected during cruise KNOX06RR represents the highest quality and quantity of data collected during a single research cruise to NER. The purpose of this research is to perform seismic stratigraphic analysis of the KNOX06RR seismic data and correlate it with drilling results to describe the stratigraphy and sedimentation characteristics along the ridge.

This thesis follows the style of *Journal of Geophysical Research.*

Geologic Setting

The NER is a ~5000 km-long, aseismic volcanic ridge trending N-S in the central Indian Ocean basin (Figure 1). This remarkably linear feature on the Indian plate extends from about 31° S at its intersection with Broken Ridge to about 10° N where it is buried beneath the sediments of the Bengal Fan (Luyendyk, 1977; Peirce et al., 1989; Royer et al., 1991). Despite its apparent continuity, the morphology of NER varies with latitude. Bathymetry data show dramatic changes from large, individual seamounts in the north, to smaller seamounts and ridges in the central region, to a high, narrow, nearly continuous ridge in the south. The ridge is about 200 km wide along most of its length, and rises 1.5 to 3 km above the surrounding seafloor. The ridge often has a asymmetric profile that is gradually sloping on the west side, plunging more steeply down on the east side into what some authors think is a deep fracture valley called the 90° Fracture Zone (Evsyukov, 2003; Luyendyk, 1977; Pilipenko, 1996) that nearly parallels the other fracture zones in the Wharton Basin to the east of NER.

Seismic reflection profiles and bathymetric data also show that NER is pervasively faulted; displaying horst and graben structures that sometimes dissect the ridge. The genesis of these morphologies is not yet understood. Some faults were likely contemporary with formation of the ridge, but others show movement related to the ongoing deformation of the Indo-Australian plate (Royer and Gordon, 1997). The age of the basement of NER was recently confirmed to follow a simple linear age progression from 43 Myo at the southern end to 77 Myo at the northern end (Duncan, 1991; Pringle et al., 2008). These results are based on new analyses of rock samples from cruise KNOX06RR and from previous suggestions of an age progression (Duncan, 1991; Royer et al., 1991).

Formation of NER

Many hypotheses regarding the formation of the Ninetyeast Ridge have emerged since its discovery in the early 1960s. It has been suggested that the ridge is a segment of uplifted oceanic crust (Francis and Raitt, 1967; Laughton et al., 1970; Royer et al., 1991), result of hotspot interaction with the Wharton spreading center (Krishna et al., 1999; Luyendyk, 1977; Royer et al., 1991; Veevers et al., 1971), or was emplaced by a leaky transform fault (Luyendyk, 1977; Neprochnov et al., 2000; Royer et al., 1991). The most widely accepted hypothesis is that of formation by a single hotspot due to the northward drift of the Indian Plate during the Late Cretaceous and Cenozoic, which fits the ridge's age progression (Krishna et al., 1999; Royer et al., 1991; Sager et al., 2007).

Sedimentation on NER Known from Previous Studies

DSDP and ODP have contributed most of the lithologic and stratigraphic data for the NER. Drilling results throughout the Indian Ocean have shown that several factors affected its distribution of sediments. The sedimentation of the NER has been influenced by terrigenous and basin sedimentation processes and ocean circulation patterns (Davies and Kidd, 1977).

Major tectonic events such as uplift and erosion of the Himalayas and subsequent creation of the Bengal sediment fan have affected terrigenous sedimentation along the ridge (Davies and Kidd, 1977). The northernmost site of this study, ODP Site 758, lies within the Bengal Fan. Drilling results report dilution of the carbonate sediment in the upper 100 MBSF, by terrigenous clay from the Bengal Fan, likely of Himalayan origin (Peirce et al, 1989). The sites south of ODP 758 lie outside of the Bengal Fan and therefore outside the proximity of terrigenous sedimentation.

Davies and Kidd (1977) report that high equatorial sea surface productivity in the Indian Ocean, as in the other major oceans, is also a factor which affected sediment supply to the NER as sites crossed the equator during the northward drift of the Indian plate and ridge formation. Indian Ocean circulation, especially the strength of its bottom currents and their ability to dissolve siliceous and carbonate sediments, has changed through time with the tectonic evolution of the Indian Ocean basins (Davies and Kidd, 1977).

Each of the four drill sites along the NER included in this study exhibit a variable succession of sedimentary and volcanic lithologies overlying igneous basement. ODP drilled Site 758 at 5° 23' N to a depth of 677 MBSF and identified five major lithologic units: Nannofossil ooze overlies chalk and volcanic clay followed by tuff and 77 Myo basalt basement (Peirce et al., 1989; Pringle et al., 2008). DSDP drilled Site 216 at 1° 27.73' N to a depth of 477.5 MBSF and identified three major lithologic units: A thick unit of nannofossil ooze and chalk overlies a unit of volcanic clay and chalk interbedded with ash. The underlying unit is basalt basement dated at 72 Myo (Pringle et al., 2008; von der Borch et al., 1974). DSDP drilled Site 214 at 11° 20' S to a depth of 500 MBSF and identified five major lithologic units: A thick unit of nannofossil ooze and chalk overlie a unit of carbonate silt and sand with some shells and volcanic components. Above the 62 Myo basalt basement lie alternating layers of volcaniclastics interbedded with lignite and find-grained basalt (Pringle et al., 2008; von der Borch et al., 1974). DSDP drilled Site 253 at 24° 52.65' S to a depth of 559 MBSF and identified four major lithologic units: nannofossil ooze and chalk overlie volcanic ash and basalt above basalt basement dated at 48 Myo (Davies et al., 1974; Pringle et al., 2008).

This study compares modern, high resolution seismic data to lithology to better understand sedimentary layers, thickness, and nature of basement of NER. The findings of this study are a compilation and elucidation of what was found by DSDP and ODP during their site surveys and drilling of NER at Sites 214 and 216 (Leg 22), 253 (Leg 26), and 758 (Leg 121) and show that despite the large separation between drill sites along the ridge, a similarity between the lithologic units and sedimentary history can be drawn.

CHAPTER II

DATA AND METHODS

Acquisition

The data for this study were acquired during the cruise KNOX06RR, a site survey cruise for proposed drilling aboard the R/V *Roger Revelle* in 2007. During the 47 day cruise, a suite of geological and geophysical data, including seismic reflection profiles, multibeam bathymetry, chirp echo-sounder profiles, gravity and magnetic data, and dredged rock samples were collected.

More than 3700 km of high-resolution 2D seismic reflection profiles were collected at seven sites (Site 758, 216, NER2, NER3, 214, NER4, and 253) along the NER between 5.5° N and 28.1° S latitude (Figure 1). Seismic survey sites were chosen primarily based on proximity to existing Deep Sea Drilling Project (DSDP) and Ocean Drilling Program (ODP) drill holes (Sites 758, 216, 214, and 253) for interpretation and correlation with existing lithologic data. The multichannel (10-fold) seismic data were collected using an array of two identical generator/injector (GI) air guns (45 in3/105 in3) with a 48-channel streamer having a receiver group interval of 12.5 m (Table 1).

Processing

The seismic data were processed using Landmark ProMAX® software (v.2003.19.1). Each 9-second record was quality checked for dead shots and traces. The acquisition geometry (shooting direction, number of shots, ship speed, depth of streamer and guns, group interval) was applied to the data in order to accurately assign common depth points (CDPs).

The data were then filtered using an Ormsby (cosine taper) bandpass filter to a level dependent on the severity of the noise level. Typical low-pass filter values ranged from 15-25 Hz and a high-pass value of 500 Hz was used consistently throughout the data. Velocity analysis was performed on the data to determine stacking velocities. Normal Moveout Correction (NMO) was applied and the data were stacked. The data were then time-migrated using a constant 1500 m/s interval velocity. Finally, the water column was muted out to give the data a cleaner appearance for viewing and interpretation.

Interpretation

Seismic data were interpreted with SMT KINGDOM software (v. 8.1) using standard seismic stratigraphy principles (Mitchum et al., 1977). Three major horizons, including acoustic basement, were interpreted based on distinct acoustic properties of reflectors including amplitude and wavelength, as well as the continuity and geometry of reflectors which can suggest changes in lithologic type. These three horizons were consistent at all sites. A number of strong (high acoustic impedance contrast) reflectors were not interpreted as horizons because they were either not sufficiently continuous or because they did not correspond to a boundary between reflectors with distinct acoustic properties. Horizons were correlated with the major reflectors published for the corresponding DSDP and ODP documentation, and extrapolated out to the surrounding area on the ridge.

Three seismic units are defined, Seismic Units I, II, and III, and are marked at the top by the major horizons that overlie them. By categorizing the seismic data into units using the DSDP and ODP drill core data as a ground-truth, we can interpret the sedimentary layers at great distances away from the drill sites. The uppermost unit, Seismic Unit I, comprises a sequence of low amplitude (sometimes nearly transparent), high frequency reflectors that are mostly uniform in their amplitude and wavelength. These reflectors have an overall draped appearance, suggesting sediments deposited in a pelagic environment. This seismic unit includes nannofossil and foraminifer ooze and along with chalk at certain sites.

The second unit, Seismic Unit II, is characterized by reflectors with variable amplitude and frequency, with transparent patches throughout. The base of this unit is generally marked by a nearly transparent band. This unit is not ubiquitous, but does appear to some degree of thickness at each of the seven sites. In DSDP and ODP cores, this unit comprises the following lithologies: chalk, volcanic clay with foraminifers or chalk, tuff with basalt pebbles, shells, ashy calcareous chalk interbeds, glauconitic carbonate silt and sand, volcaniclastics, and basalt.

The last unit, Seismic Unit III, marks the top of acoustic basement and represents volcaniclastics and basalt. This unit is distinguished from Seismic Unit II by a large acoustic impedance contrast visible in a set of reflectors of variable amplitude and frequency, generally higher in amplitude and lower in frequency. Reflectors in this unit are typically discontinuous and highly chaotic, in many places likely corresponding to a lithologic change to basalt, marking igneous basement. Given the size of the seismic source, the degree to which igneous basement is imaged is variable depending on factors such as depth to the top of the ridge and the thickness of the sediment column.

Depending on the depth of acoustic penetration in a given area, one of the three following scenarios exists: (1) acoustic basement occurs *above* the igneous basement because igneous basement was not imaged below the overlying volcanic sediment column; (2) acoustic basement coincides to igneous basement. (3) acoustic basement occurs *below* igneous basement because acoustic wave penetration was great. In any of the three scenarios, the acoustic basement horizon was mapped and the seismic unit below was defined accordingly as basement.

Correlation of seismic data with lithologic units from drill cores was made for the sites with drilling results (ODP 758, DSDP 216, DSDP 214, and DSDP 253; von der Borch et al., 1974; Davies et al., 1974; Peirce et al., 1989). Averages of published DSDP and ODP velocities were used to estimate the depths to lithologic contacts and major reflectors in order to correlate those depth values to time values on the seismic data. An estimated conversion of depth (m) from TWTT (s) was made by first dividing the time to each of the major horizons by 2 since the data are in TWTT (s). The one way travel time value was then multiplied by the velocity measured for the rock samples cored to yield a depth in meters below the sea surface at each of the three major horizons.

Isopach maps of total sediment thickness and distribution were generated using SMT Kingdom software by subtracting the TWTT to the seafloor horizon from the TWTT to the basement horizon, thereby creating an isopach to portray the depth (in time) of the sediment column. These isopach values were gridded in the software using the cubic spline method and then contoured to create the final maps. A velocity of 1500 m/s was used to convert time (s) to depth (m) for all interpretations of depths to horizons, size of features, and thickness of units. Seismic survey tracks are widely spaced in many areas forcing the contouring software to interpolate isopach values between tracklines and extrapolate isopach values beyond where tracklines end. Consequently, the isopach values are most reliable nearest ship tracklines. All seven sites have an estimated minimum sediment thickness of essentially zero since there is at least one basement outcrop at each site.

CHAPTER III

OBSERVATIONS AND RESULTS

Site Descriptions

KNOX06RR Site 758. This site (Figure 2) covers the southern flank of a large seamount and two smaller seamounts at the northernmost end of NER. It contains ODP Site 758 at 5° 23.049' N, 90° 21.673' E (Peirce et al., 1989). At this latitude, NER is made up of large, individual seamounts. The bathymetry data show that the top of the ridge is at ~3 km depth. The sediment column has a maximum thickness of 0.778 s (~580 m; Figure 3). Sediment is thickest at the northeast extent of the site where the steep-walled SW-NE trending canyon on the eastern scarp of the ridge appears in the seismic data to be transporting sediment to the abyssal plain (Figure 2, 4). The thinnest sediment at this site is atop the tallest seamount and large adjacent seamount to the southeast; it thins to 0.026 s, or ~19 m in places on their tops and flanks, and is occasionally absent where faulting has exposed basement. Furthermore, sediment is thin east of ODP Site 758 where the wedge of sediment seen in Figure 4 pinches out at the edge of the plateau just west of the aforementioned canyon. The thickness of the sediment column at the position where ODP Site 758 was drilled is 0.532 s, nearly 500 m (Peirce et al., 1989).

Figure 4 shows a W-E seismic profile along 5° 23' N (Figure 2), which crosses ODP Site 758. The uppermost unit of seismic reflectors at this site, Seismic Unit I, is a sequence of low amplitude, high frequency reflectors, sometimes nearly transparent, with an overall draped appearance. Reflectors are generally continuous and conformable, though they appear chaotic in places as depth increases. Seismic Unit II is marked by a shift to reflectors with moderate and constant amplitude and frequency, with occasional transparent patches. The base of this unit is generally marked by an acoustically transparent band. The acoustic basement horizon and Seismic Unit III is marked by a large acoustic impedance contrast visible in a set of reflectors of variable amplitude and continuity, but that have generally higher amplitude and lower frequency. This set of reflectors quickly becomes transparent due either to signal attenuation or a lack of change in physical properties within the unit, suggesting that the acoustic basement reflector also marks the top of igneous basement. Figure 4 shows that the reflectors in Seismic Unit I and II pinch out above basement from west to east suggesting multiple periods of erosion as these layers were laid down. Seismic Data in Figure 2 and bathymetric data in Figure 4 also show that basement outcrops along the steep walls of the SW-NE trending canyon that is carved into Seismic Units I and II.

KNOX06RR Site 216. Just north of the equator on a large oblong seamount, this survey covered the top and eastern flank of NER and crossed DSDP Site 216 at 1° 27.73’ N, 90° 12.48’ E (Figure 5; von der Borch et al., 1974). The bathymetry data show that the depth to the top of the ridge is 2-2.5 km. The eastern flank of NER here is characterized by a scarp of variable steepness. Directly east of DSDP Site 216, just off the eastern scarp of the ridge, there is a single seamount and a smaller mound adjacent to it to the southeast. There are several areas of thin sediment across this survey site. The thinnest sediment occurs in areas of basement highs where sediment appears to have preferentially accumulated on the lower surrounding areas, but forms a thinner drape between 0.171-0.217 s (<200 m thick) on the high areas. Sediment is absent on the volcanic cone (Figure 5) on the east flank and where basement is exposed on the eastern scarp of the ridge as sediment from above has slumped or moved down slope through mass wasting. The greatest thickness of the sediment column at this site is 0.775 s (~580 m; Figure 6), just north of DSDP Site 216, where the basement is slightly lower and layered sediments have accumulated. Figure 16 shows a N-S seismic profile along 90° 12.5’ E at (Figure 7), which crosses DSDP Site 216. Reflectors at this site have generally the same the same acoustic characteristics as at Site 758, with a largely transparent Seismic Unit I at the top and a more reflective package of reflectors as Seismic Unit II in the lower sediment column. Figure 7 shows that the reflectors in Seismic Unit II onlap the acoustic basement horizon to the north, suggesting either basin fill or a northward direction of deposition onto the basement high. The figure also shows that the reflectors in Seismic Unit I, just north of DSDP Site 216, remain conformable for many kilometers except where dissected by a major fault.

KNOX06RR Site NER2. This survey covered the top and western flank of a seamount between 6° 15’ S and 7° 10’S. In this area, the ridge changes morphology from a large, wide seamount chain to a long, narrow, and linear ridge (Figure 8) with a steep western flank. The bathymetric data show that the depth to the top of the ridge at this site between 2.75-3 km. Seismic and bathymetric data show a seamount at the north end of the site that is nearly bare of sediment. At KNOX06RR Site NER2, the maximum thickness of the sediment column is 0.728 s, up to 546 m (Figure 9) where the seismic data show a faulted and undulating basement surface that has created accommodation near the center of the site (Figure 10). This zone can be seen in the bathymetry as a broad, E-W trough across of the ridge (Figure 8). Areas of thin sedimentation occur at the northernmost and southernmost extents of the site (Figure 9). In the north, the two basement highs are bare or nearly bare on their flanks, and capped with very little sediment (0.096 s, <100 m). Figure 10 shows a W-E seismic profile along 6° 43’ S where there is good definition of the three seismic units. Along this transect on the top of the ridge, the reflectors within Seismic Units I and II are generally conformable and follow the gentle undulation of the basement surface, though there isn't always a transparent band of reflectors directly above the acoustic basement reflector. The basement reflectors of Seismic Unit III are very chaotic, and produce a large acoustic impedance contrast. There are some places where the basement reflectors display a layered appearance, as if from volcanic flows or volcaniclastic sediments. At the center of the site, there is an area of thin sediment, where seismic data show there is a basement high in which the reflectors above basement clearly downlap on the basement reflector. In various seismic profiles across the site, reflectors in Seismic Unit II show a combination of downlap and onlap onto the Seismic Unit III, a clear distinction between basement and the overlying sedimentary layers.

KNOX06RR Site NER3. This survey also covered the top and western flank of NER between 7° 10'S and 8° 10' S on the same segment of the ridge as Site NER2 (Figure 11). Bathymetric data show that the depth to the top of the ridge at this site between 2-2.5 km. This site is separated from Site NER2 by a graben nearly 17 km wide and more than 1200 m deeper than the top of the ridge, oriented in an E-W direction (Figure 8). The graben has bare walls, but 0.321 s (>200 m) of sediment has accumulated at the bottom. The thickness of the sediment column is up to 0.908 s (681 m; Figure 12) on the western flank of the ridge, sediment is accumulated on what appears to be the maximum angle of repose of the ridge. At the southern end of the site there is another area of thick sediment accumulation of 0.87 s, which is more than 650 m. The sediment is either thin or absent on both the eastern and western flanks of the ridge. The western flank is steep and devoid of sediment. The eastern flank is nearly as steep and is covered by 0.031 s (~23 m) of sediment. Figure 13 shows a N-

S seismic profile along 88° 59' E (Figure 11) on a low-lying area on the crest of the ridge. Seismic data across the survey site exhibit large relief in the reflectors in all three seismic units, and many large scale faults dissect the basement and intersect and deform the overlying units.

KNOX06RR Site 214. This site covers much of the width of NER, including DSDP Site 214 at 11°20.21' S, 88° 43.08' E (Figure 14; von der Borch et al., 1974). At this latitude, the NER is a wide, long, and linear ridge. Bathymetric data show that the depth to the top of the ridge here is ~1.5 km. Seismic data show that the maximum thickness of the sediment column occurs at the north end of the site approximately half-way up the ridge crest where there is a shelf in the basement and sediment has accumulated to 0.949 s (~712 m). A N-S seismic profile along 11° 15'S, thick sediment 0.795 s (nearly 600 m thick) has accumulated at the base of the eastern slope of the ridge. Sediment is either absent or no thicker than 10 m at the perimeter of the site along the eastern flank of the ridge where the slope is too great to accumulate sediment. The slightly gentler slope on the west side has accommodated sediment coverage of 0.084 s (~100 m) in places. Figure 16 shows a N-S seismic profile along 88° 43' E (Figure 14) which crosses DSDP Site 214 at 11° 20.21' S (von der Borch et al., 1974). Seismic data show that basement is pervasively faulted with high angle faults primarily in the E-W direction. The acoustic basement reflectors are very strong, though there is a less obvious distinction between Seismic Unit I and II as in the previous sites. Many of the faults create half-grabens in the basement surface and the reflectors in the overlying units appear to fill them in. However, since many of the large faults that affect basement do not extend to the seafloor, the reflectors in Seismic Unit I are not affected nearly as much as those in Seismic Unit II, suggesting faulting early in the ridge’s history. At this site, the distinction between Seismic Unit I and II comes in many places from the changes in the stratal relationship of the reflectors rather than changes in their acoustic properties.

KNOX06RR Site NER4. This site covers the top and eastern flank of NER and the fracture zones east to 89 °, between 19° and 20° S (Figure 17). This site is on the same ridge segment as Site 214. Along the 167 km transect, sediment thickness is quite variable. On the west side of the site a large, NE-SW trending graben (Figure 17) exposes basement on its walls, but is filled with sediment to a thickness of 0.967 s (~725 m). The sediment is considerably thinner along this transect to the east, where the fracture zone ridges leave basement exposed, but fracture zone troughs are filled with sediment as thick as 0.39 s (~300 m). Figure 18 shows a W-E seismic profile along 19° 18’ S (Figure 17). Seismic reflectors at this site are very chaotic from the seafloor all the way through basement. Reflectors indicate that sediment thins considerably from the top of the ridge to the flank. Seismic Unit I and III are fairly well distinguished at this site, but Seismic Unit II is only seen as a continuous unit for a short distance at the eastern edge of the ridge and is not clearly defined. The basement horizon is very clearly defined at this site as the data show good penetration for considerable depth in some places. The highly faulted basement surface is well imaged at the east of the site in the fracture zones as can be seen in Figure 18.

KNOX06RR Site 253. The survey covered the top and eastern flank of NER in proximity to DSDP Site 253 at 24° 53’ S, 87° 22’E (Figure 19, Davies et al., 1974). This site is on the southernmost segment of NER where it is wide, flat-topped, and linear. The bathymetry data show that the depth to the top of the ridge here is ~2 km. The maximum thickness of the sediment column is up to 1.047 s (Figure 20) and occurs near the middle of the site where seismic data reveal a graben that has created accommodation for ~785 m of sediment. There are multiple areas of thin or absent sediment; the ridge is bare on the scarps of the various horsts that make up the site. On the southwest side of the site, the edge of the ridge exhibits large-scale normal faulting which has created horsts and grabens devoid of sediment on their walls and very little blanketing their tops. At the northern, eastern, and southeastern extent of the site, various volcanic peaks and cones that at the edge of the ridge are bare of sediment. Figure 21 shows a N-S seismic profile along 87° 44’ E (Figure 19). No new seismic or bathymetric data were collected over DSDP Site 253 at 24° 53’ S, 87° 22’ E, but drilling results showed that depth to volcanic basement is 559 m (Davies et al., 1974).

Seismic data show clear definition of all the seismic units and a highly faulted basement surface. The reflectors in Seismic Unit I are clearly defined low amplitude, high frequency reflectors that are generally conformable with the horizon for Seismic Unit II. Seismic Unit II is interpreted throughout most of the site, but its reflectors coalesce with those in Seismic Unit I at the base of slopes and volcanic cones. Basement is clearly imaged at this site, especially where sediment is thin allowing for more energy to penetrate the basement surface, and where basement outcrops on the seafloor as volcanic cones.

Correlation of Seismic Reflection Profiles with Drilling Results

Seismic stratigraphic interpretations were made using seismic profiles from the four survey sites that crossed DSDP or ODP drill sites, with the exception of DSDP Site 253 in which the nearest seismic profile is nearly 60 km away. Times to horizons are given where profiles cross DSDP or ODP drill sites only, and estimated for 253. KNOX06RR Sites

NER2, Site NER3, and Site NER4 have no drilling results to correlate to the seismic reflection profiles.

KNOX06RR Site 758. The seismic reflection profile chosen for correlation with drilling results (Figure 22) is a W-E profile across the ODP Site 758 drill hole (Figure 2, 4). Three major horizons were interpreted at 3.945 s (seafloor reflector), 4.234 s, and 4.478 s two-way travel time (TWTT). The first horizon corresponds to the seafloor and the top of Seismic Unit I, the pelagic sequence of nannofossil ooze and chalk of Holocene to middle Miocene age (Peirce et al., 1989). The second major horizon lies within a late Paleocene age chalk layer with chert nodules, the latter being the likely the source of the strong acoustic impedance contrast (Peirce et al., 1989). This horizon represents the top of Seismic Unit II at a depth of ~270 meters below seafloor (MBSF). Seismic Unit II includes the following lithologies: chalk, chert, volcanic clay, ash, and basalt. The last major horizon represents acoustic basement and the top of Seismic Unit III. This reflector corresponds to a depth of ~567 m below seafloor, likely corresponding to the top of the Campanian (~77 Myo) basalt basement (Duncan et al. 1991; Peirce et al., 1989; Pringle et al., 2008).

KNOX06RR Site 216. The seismic reflection profile chosen for correlation with drilling results (Figure 23) is a S-N profile across the DSDP Site 216 drill hole (Figure 5, 7). Three major horizons were interpreted at 3.059 s (seafloor reflector), 3.347 s, and 3.489 s. The first horizon corresponds to the seafloor and the top of Seismic Unit I, the pelagic sequence of nannofossil ooze and chalk, Pleistocene to late Oligocene age (von der Borch et al., 1974). The second major horizon occurs at a depth of ~300 MBSF and marks the top of Seismic Unit II which lies within the nannofossil ooze and chalk, most likely caused by chert stringers within the nannofossil chalk. Seismic Unit II includes nannofossil ooze with chalk and chert stringers, glauconite, and volcanic clay, chalk, and ash, and ranges in age from Late Oligocene to late Maastrichtian in age (von der Borch et al., 1974); the top of the unit likely corresponding to a layer of Paleocene chalk. The last major horizon represents acoustic basement and the top of Seismic Unit III. This horizon correlates well with the boundary between the volcanic clay/chalk/ash and basalt at a depth of ~450 MBSF. The age of volcaniclastics was reported as Late Maastrichtian in age and the age of the basalt is ~72 Myo (Duncan, 1991; Pringle et al., 2008; von der Borch et al., 1974)

KNOX06RR Site 214. The seismic reflection profile chosen for correlation with drilling results (Figure 24) is a W-E profile across the DSDP Site 214 drill hole (Figure 14, 16). Three major horizons were interpreted at 2.266 s (seafloor reflector), 2.618 s, and 2.695 s. The first horizon corresponds to the seafloor and the top of Seismic Unit I; the pelagic unit of Pleistocene to Paleocene nannofossil ooze (von der Borch et al., 1974). The second major horizon marks the top of Seismic Unit II at ~334 MBSF and correlates well with the boundary between the nannofossil ooze and glauconitic carbonate silt and sand of Paleocene age (von der Borch et al., 1974). The third major horizon which marks acoustic basement occurs at a depth of ~407 MBSF, within a sequence of alternating volcaniclastics interbedded with lignite and basalt (von der Borch et al., 1974). Duncan et al. (1991) and Pringle et al. (2008) showed that the age of basalt at this site is ~62 Myo.

KNOX06RR Site 253. The seismic reflection profile chosen for correlation with drilling results (Figure 25) is a S-N profile in the vicinity of DSDP Site 253 to the NW (Figure 19 and 21). Three major horizons were interpreted at 2.274 s (seafloor reflector), 2.480 s, and 2.761 s. The seismic survey at this site was conducted approximately 60 km from DSDP Site 253 drill site. A location representative of the stratigraphy at the drill site was chosen on a line nearest the drill site for seismic stratigraphic correlation. As such, stratigraphic seismic correlations are speculative at best. The first horizon corresponds to the seafloor and the top of Seismic Unit I, nannofossil ooze and chalk sequence of Quaternary to middle Eocene age (Davies et al., 1974). The second major horizon marks the top of Seismic Unit II and occurs at a depth of ~158 MBSF and likely correlates to a chalk layer below the nannofossil ooze. The last major horizon occurs at a depth of ~565 MBSF, and the top of Seismic Unit III. This reflector represents acoustic basement and correlates well with the contact between volcanic ash and basalt which is ~48 Myo (Davies et al., 1974; Duncan, 1991; Pringle et al., 2008).

CHAPTER IV

DISCUSSION

There are several factors outside the scope of this study that may have affected the sedimentary history of NER. KNOX06RR collected seismic reflection profiles at seven sites along the 5000 km NER, only four of which are correlatable with DSDP and ODP drill sites. Given more closely spaced drill cores available for a ground-truth of lithologies, a more accurate picture can be drawn of the sedimentary history of NER. Currents in the Indian Ocean have undoubtedly played a role in the deposition of sediments on NER through time. The present day circulation in the Indian Ocean is counterclockwise, though may have had different directions as the Indian Ocean basin evolved to its present configuration. There is some degree of influence by the Bengal sediment fan on the sedimentation of the northern end of NER especially at Site 758 (Peirce et al., 1989) but the extent of which has not been investigated in this study. The precise subsidence rate of NER was not examined here, but because the depth to the carbonate compensation depth (CCD) is deeper than the ridge at ~4700 m (Peirce et al., 1989) sediments would not have been affected.

Three major horizons were interpreted throughout the seismic data along NER, correlated with those previously recognized at the DSDP and ODP sites, and categorized into three seismic units based on distinct acoustic properties. Seismic Unit I was shown to comprise a succession of pelagic sediments and sedimentary rock draped over Seismic Unit II, which consists of pelagic carbonates mixed with volcaniclastics. Seismic Unit III is volcanic basement (von der Borch et al., 1974; Davies et al., 1974; Peirce et al., 1989).

Given the known ages of the major lithologic units at the drill sites as published by DSDP and ODP, and the progressive igneous basement ages from 77 My at the northernmost end of NER to 43 My at the southernmost end of NER, we can begin to understand the sedimentary history of NER since its formation. The major lithologic units drilled at each site indicate their depositional environment.

At the northern, oldest (77 Myo) end of the ridge at site 758, drilling results indicate the volcanic basement and the sediment overlying it were deposited in an open marine pelagic environment. The uppermost lithologic unit on the ridge is nannofossil ooze which was deposited in deep marine (pelagic) environment (Duncan, 1991; Peirce et al., 1989; Pringle et al., 2008). At Site 216 the 72 Myo basalt basement and the overlying volcaniclastics were deposited in shallow submarine eruptions, and the chalk was deposited in shallow water environment whereas the nannofossil ooze was deposited in a pelagic environment (von der Borch et al., 1974, Duncan, 1991; Pringle et al., 2008). von der Borch et al. (1974) indicate that at Site 214 the 62 Myo basalt basement and overlying volcaniclastics were emplaced either in subaerial or shallow marine eruptions and that this site was an island during time of formation. The carbonate silt and sand were deposited in shallow marine, perhaps lagoonal environment given the presence of lignite. The nannofossil ooze was deposited in an open marine pelagic environment (von der Borch et al., 1974). At the southern end of the ridge at the youngest (48 Myo) study site, basalt basement was emplaced by submarine eruptions at or near sea level (Davies et al., 1974; Duncan, 1991; Pringle et al., 2008). The volcanic ash was deposited in subaerial or submarine and the chalk and nannofossil ooze were deposited in submarine relatively shallow ~1020 m (Davies et al., 1974; Duncan, 1991; Pringle et al., 2008).

Based on drilling results, the paleo-depth of the ridge at time of emplacement became shallower with time, ranging from submarine to subaerial volcanic eruptions followed by subsidence to pelagic depths, determining the depositional environment on the ridge post-emplacement. Given the present depth to the top of the ridge we know that the ridge has subsided through time, resulting in the northern sites on the ridge remaining deeper than the southern sites. When correlated, the seismic, bathymetric, and core data indicate a common sedimentary history at each site: volcaniclastic-rich sediments deposited during or shortly after ridge formation topped by a thick drape of pelagic sediments. This history likely happened in three stages over the last ~77 My: 1) the initial subaerial or submarine emplacement of the volcanic ridge, 2) the deposition of shallow water sediments and volcaniclastics, and finally 3) the subsidence of the ridge followed by deep water pelagic sediment deposition.

CHAPTER V

CONCLUSIONS

More than 3700 km of new 2D multichannel seismic reflection profiles collected in 2007 show details of sediment layers, basement surface, and faulting along the NER. Stratigraphy and sediment thickness along the ridge using were studied using these new seismic data, published lithologic data from DSDP and ODP cores, and new basement age data, in order to describe the sedimentary history of NER. New bathymetric data were correlated with seismic data to interpret and describe geologic features.

Three major horizons were interpreted throughout the seismic data and were categorized into three seismic units based on distinct acoustic properties of the reflectors. Total sediment thickness and distribution were mapped at each site (758, 216, NER2, NER3, 214, NER4, and 253) along the ridge showing a range from 0 m where basement outcrops on the seafloor to ~785 m at its thickest.

Seismic stratigraphic analysis and correlation with drilling results show a commonality between the stratigraphy at sites: a succession of pelagic sediments and sedimentary rock draped over Seismic Unit II, which consists of pelagic carbonates mixed with volcaniclastics. Seismic Unit III is volcanic basement (von der Borch et al., 1974; Davies et al., 1974; Peirce et al., 1989).

Seismic and core data indicate a common sedimentary history at each site: volcaniclastic-rich sediments deposited during or shortly after ridge formation topped by a thick drape of pelagic sediments. This history likely happened in three stages over the last ~77 My: 1) the initial subaerial or submarine emplacement of the volcanic ridge, 2) the deposition of shallow water sediments and volcaniclastics, and finally 3) the subsidence of the ridge followed by deep water pelagic sediment deposition. This model of the sedimentary history of NER is consistent with the commonly accepted theory of formation of the Ninetyeast Ridge by the trace of a single hotspot in the Indian Ocean basin, and allows us to begin to understand the stratigraphy and sedimentation along the Ninetyeast Ridge through time.

REFERENCES

Davies, T. A., and R. B. Kidd (1977), Sedimentation in the Indian Ocean through time, in *Indian Ocean Geology and Biostratigraphy: Studies Following Deep Sea Drilling Legs 22-29*, edited by J. R., Heirtzler, H. M., Bolli, T. A., Davies, J. B., Saunders, and J. G. Sclater, American Geophysical Union, Washington, D.C.

Davies, T. A., B. P. Luyendyk, K. S. Rodolfo, D. R. C. Kempe, and B.C. McKelvey (1974), *Initial Reports of the Deep Sea Drilling Project*, *26*, U.S. Government Printing Office, Washington, D.C.

Duncan, R. A. (1991), Age distribution of volcanism along aseismic ridges in the eastern Indian Ocean, in *Proceedings of the Ocean Drilling Program, Scientific Results, Volume 121*, 507-517, edited by Weissel, J., Peirce, J., Taylor, E., and J. Alt, Ocean Drilling Program, College Station, TX.

Evsyukov, Y. D. (2003), Morphology of the Ninetyeast Ridge north of the equator, *Oceanology, 43*(2), 270-275.

Francis, T.J.G., and R.W. Raitt (1967), Seismic refraction measurements in the southern Indian Ocean. *J. Geophys. Res*., doi: 10.1029/JZ072i012p03015.

Gillis, G. (2009), Geophysics, *Schlumberger Oilfield Glossary*, online, last accessed 6/17/2009. http://www.glossary.oilfield.slb.com/

Krishna, K.S., D. Gopala Rao, L.V. Subba Raju, A.K. Chaubey, and V.S. Shcherbakov et al. (1999), Paleocene on-axis hot spot volcanism along the Ninetyeast Ridge: An interaction between the Kerguelen hot spot and the Wharton spreading center, *Proc. Ind. Acad. Sci. Earth Planet. Sci., 108*, 255-267.

Laughton, A. S., D. H. Matthews, and R.L. Fisher (1970), The structure of the Indian Ocean, in *The Sea*, vol. 4, edited by A.E. Maxwell, Wiley-Interscience, New York, 543-586.

Luyendyk, B.P. (1977), Deep sea drilling on the Ninetyeast Ridge: Synthesis and a tectonic model, in *Indian Ocean Geology and Biostratigraphy: Studies Following Deep Sea Drilling Legs 22-29*, edited by J. R., Heirtzler, H. M., Bolli, T. A., Davies, J. B., Saunders, and J. G. Sclater,, American Geophysical Union, Washington, D.C.

Mitchum, R. M., Vail, P.R., and J. B. Sangree (1977), Seismic stratigraphy and global changes of sea level, part 6: Stratigraphic interpretation of seismic reflection patterns in depositional sequences, in *Seismic stratigraphy-applications to hydrocarbon exploration, AAPG Memoir 26*, edited by Payton, C. E., AAPG, Tulsa, OK.

Neprochnov, Y. P., B. N. Grin'ko, and O.Y. Ganzha (2000), Crustal structure of the Ninetyeast Ridge, *Oceanology*, *40(1)*, 79-90.

Pilipenko, A. I. (1996), Fracture zones of the Ninetyeast Ridge area, Indian Ocean, *Geotectonics*, *30*, 441-451.

Peirce, J., J. Weissel, E. Taylor, J. Dehn, and N. Driscoll (1989), *Proc. ODP*, *Init Repts.*, *121*, Ocean Drilling Program, College Station, TX.

Pringle, M.S., F. A. Frey, and E. E. Mervine (2008), A simple linear age progression for the Ninetyeast Ridge, Indian Ocean: New constraints on Indian plate tectonics and hotspot dynamics, *Eos Trans. AGU*, 89(53), Fall Meet. Suppl., Abstract T54B-03

Royer, J.-Y., and R. G. Gordon (1997), The motion and boundary between the Capricorn and Australian plates, *Science*, *277*, 1268-1274, doi:10.1126/science.277.5330.1268.

Royer, J.-Y., J. W. Peirce, and J. K. Weissel (1991), Tectonic constraints on the hot-spot formation of the Ninetyeast Ridge, in *Proc. ODP*, *Sci. Res.*, *121*, 763-776.

Sager, W., F. A. Frey, M. Pringle, C. F. Paul, and A. Eisin (2007), *Ninetyeast Ridge Expedition Cruise Report*, unpublished, Department of Oceanography, Texas A&M University, College Station, TX.

Smith,W. H. F., and D. T. Sandwell (1997), Global sea floor topography from satellite altimetry and ship depth soundings, *Science*, *277*, 1956–1962.

Veevers, J. J., J. G. Jones, and J.A. Talent (1971), Indo-Australian stratigraphy and the configuration and dispersal of Gondwanaland, *Nature*, *229*, 383-388.

von der Borch, C. C., J. G. Sclater, S. Gartner Jr., R. Hekinian, and D. A. Johnson (1974), *Initial Reports of the Deep Sea Drilling Project*, *22*, U.S. Government Printing Office, Washington D.C.

APPENDIX A

FIGURES

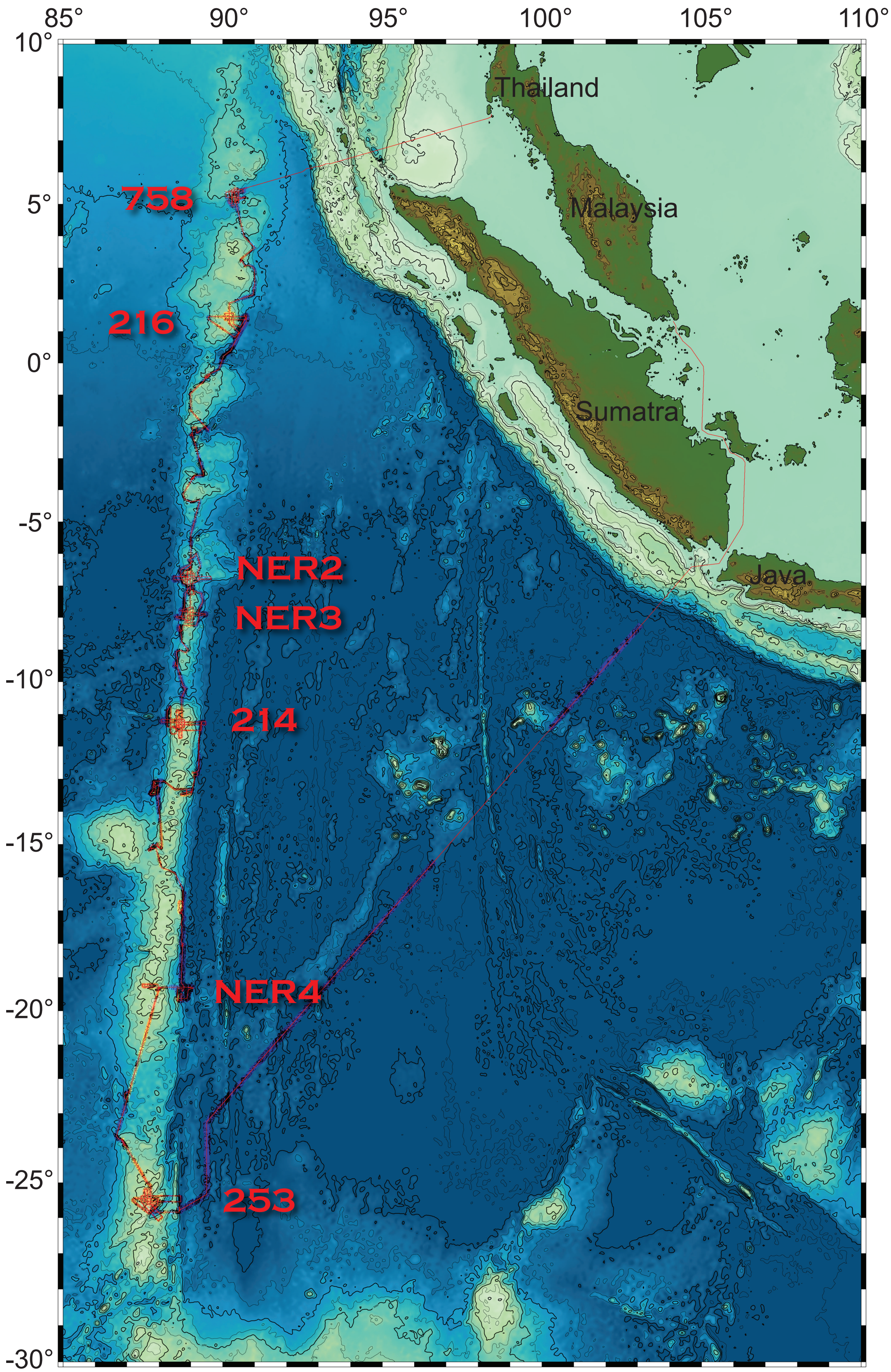

Figure 1. KNOX06RR Sitemap. Tracklines are shown in red. Red numbers indicate location of seismic survey sites. Predicted bathymetry after Smith and Sandwell (1997).

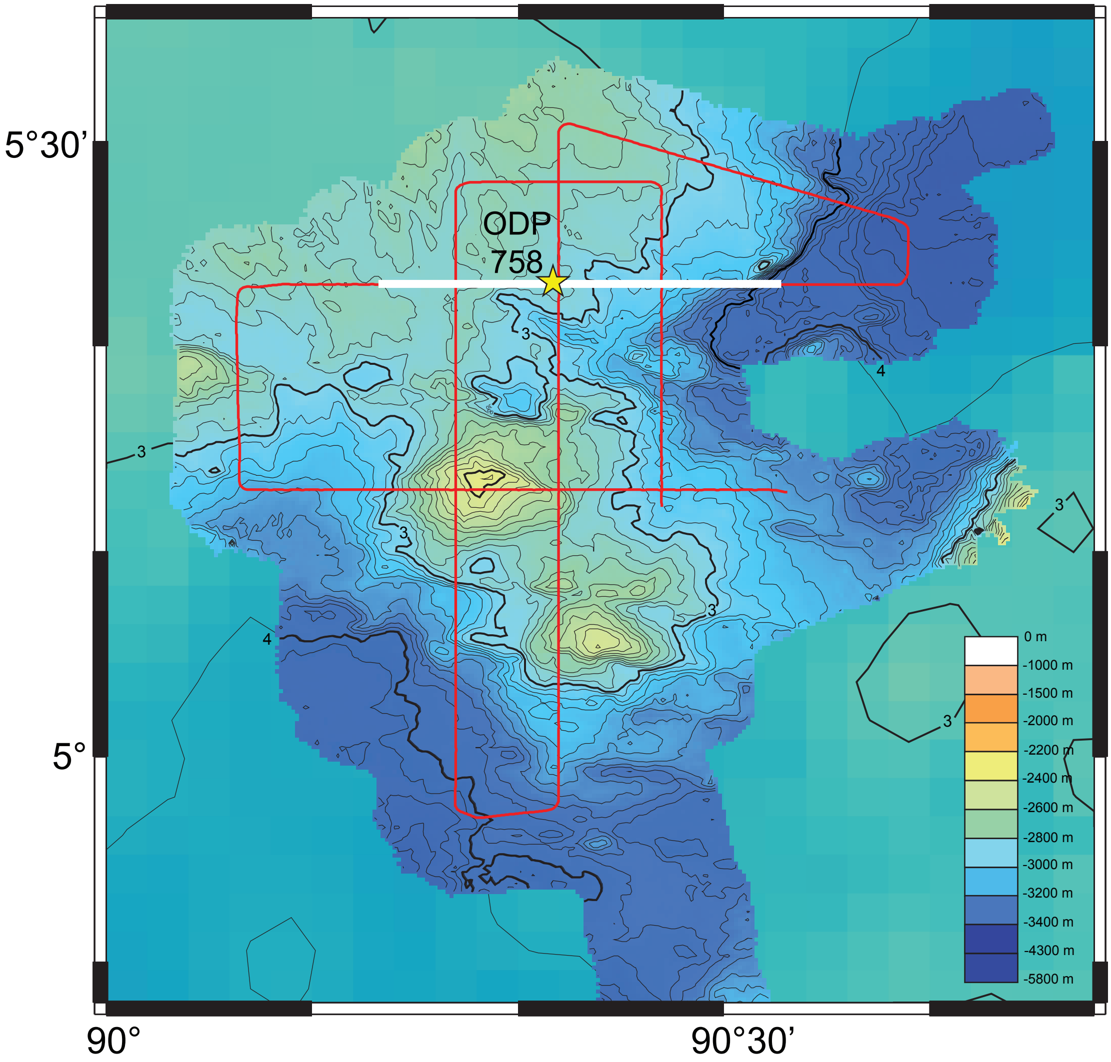

Figure 2. Seismic Survey Map of KNOX06RR Site 758. Tracklines are shown in red. White bar indicates location of seismic profile in Figure 4. Star indicates location of ODP Site 758. Multibeam bathymetry data are overlaid on predicted bathymetry (after Smith and Sandwell, 1997). Colors indicate depth with blue being deepest and warm colors shallowest. Multibeam bathymetry contour interval = 100 m. Predicted bathymetry contour interval = 1000 m.

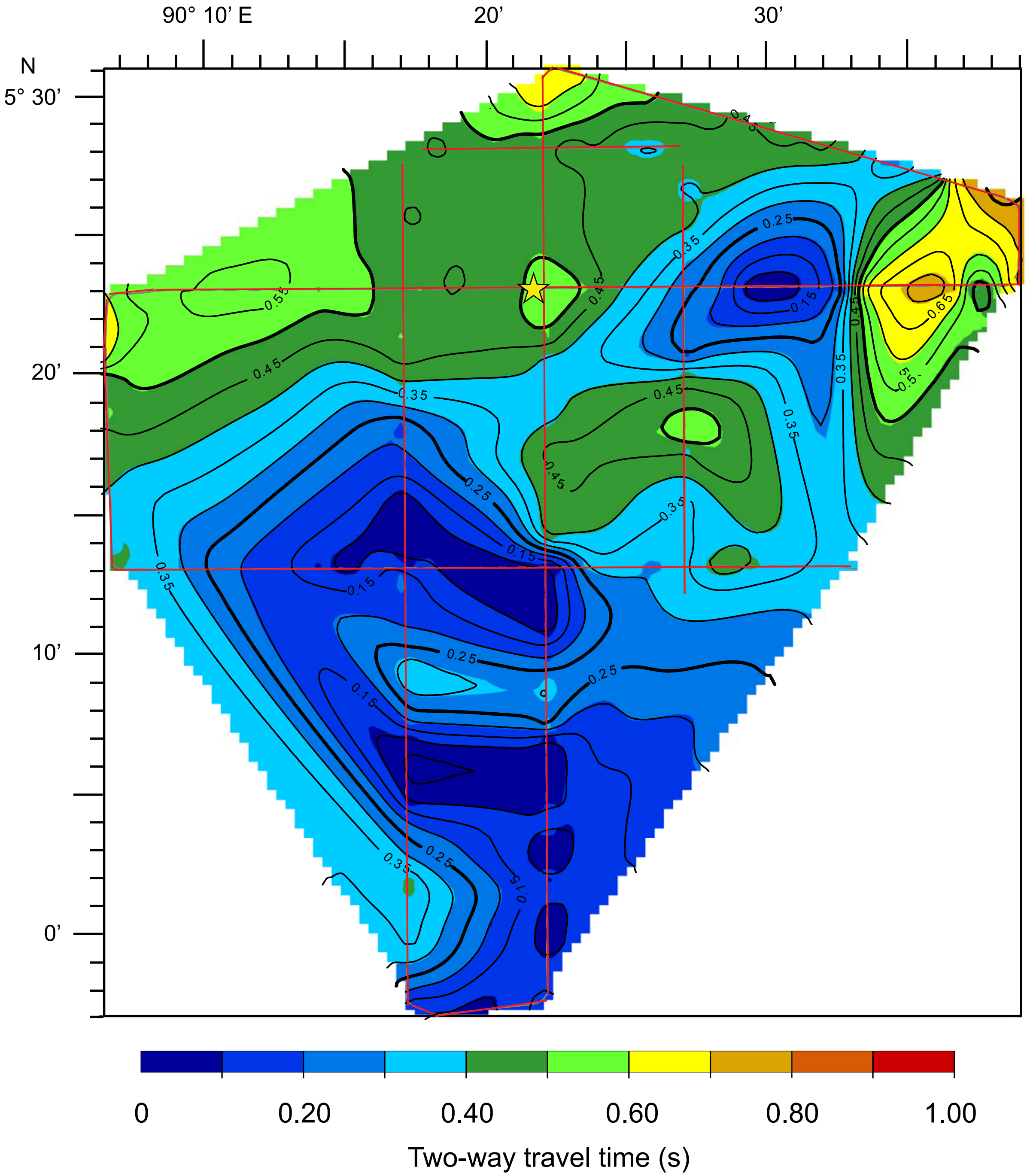

Figure 3. Total Sediment Thickness Isopach Map of KNOX06RR Site 758. Isopach represents thickness of sediment column in two-way travel time (s) between seafloor horizon and acoustic basement horizon. Contour interval = 0.05 s. Survey tracklines shown in red. Star indicates location of DSDP Site 758.

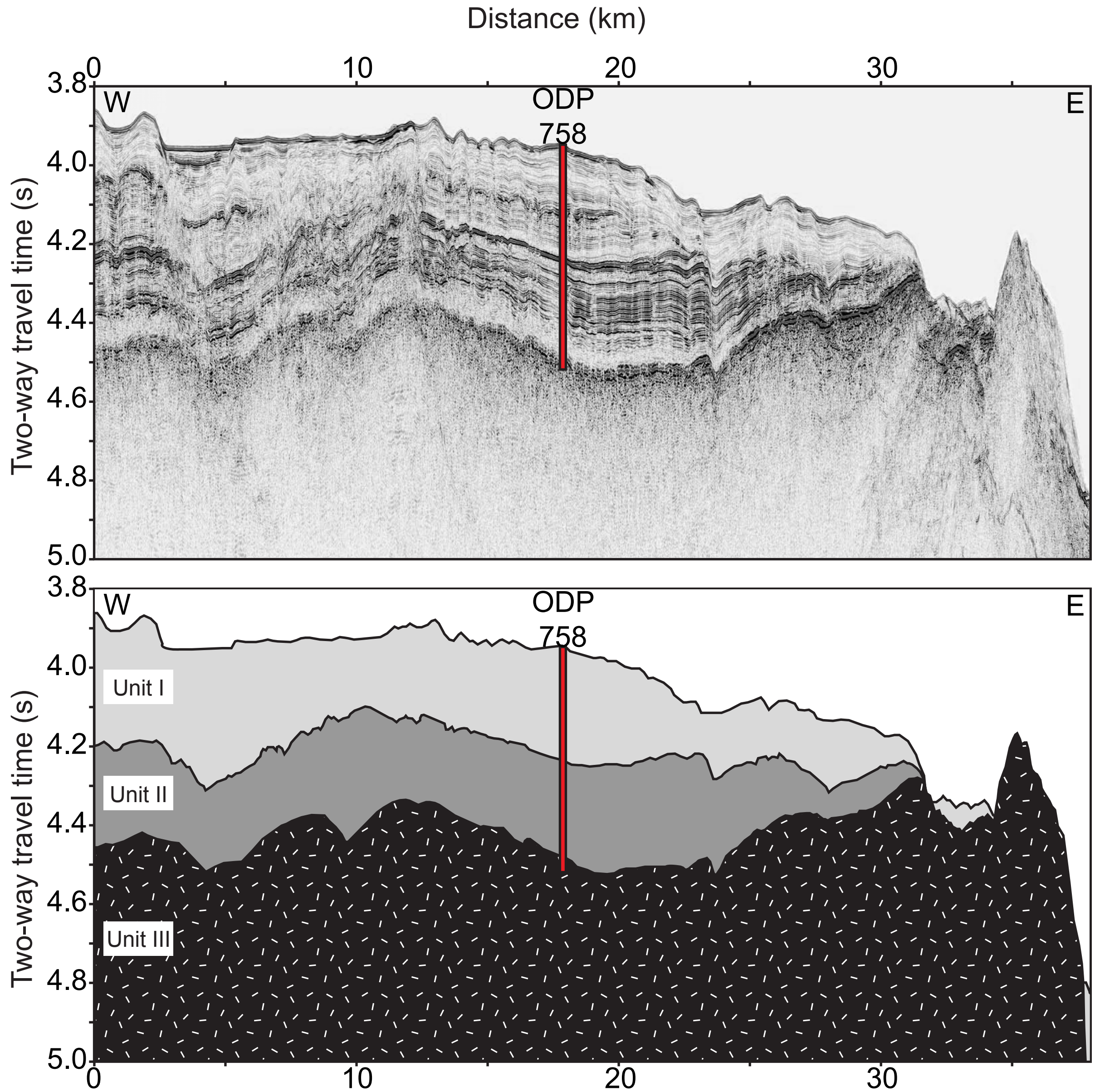

Figure 4. Seismic Reflection Profile from KNOX06RR Site 758. Uninterpreted version (top) and interpreted version (bottom) showing the division into three Seismic Units I, II, and III. Vertical red bar indicates approximate location and depth of ODP Site 758.

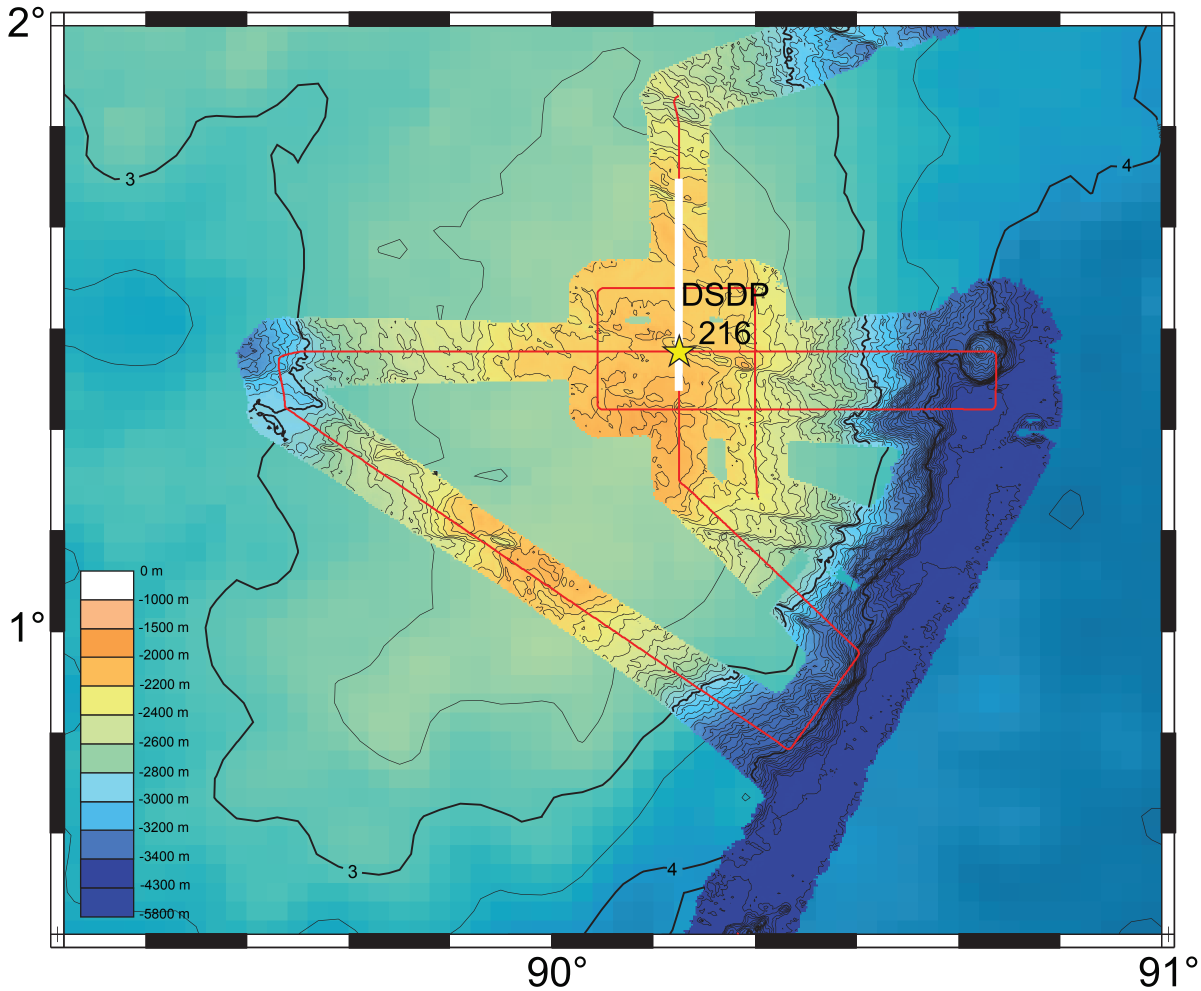

Figure 5. Seisimic Survey Map of KNOX06RR Site 216. Tracklines are shown in red. White bar indicates location of seismic profile in Figure 7. Star indicates location of DSDP Site 216. Multibeam bathymetry data are overlaid on predicted bathymetry (after Smith and Sandwell, 1997). Colors indicate depth with blue being deepest and warm colors shallowest. Multibeam bathymetry contour interval = 50 m. Predicted bathymetry contour interval = 500 m.

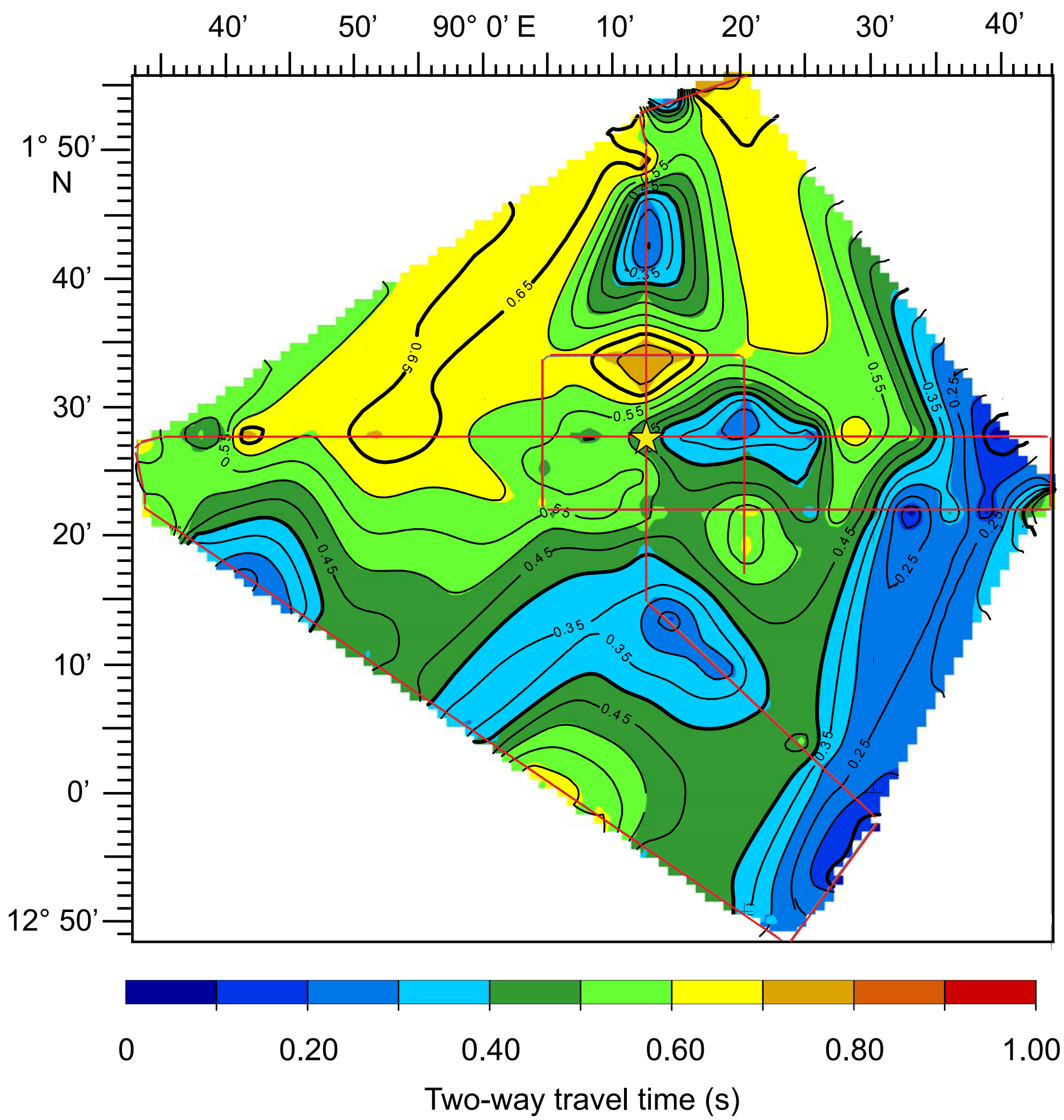

Figure 6. Total Sediment Thickness Isopach Map of KNOX06RR Site 216. Star indicates location of DSDP Site 216. Conventions as in Figure 3.

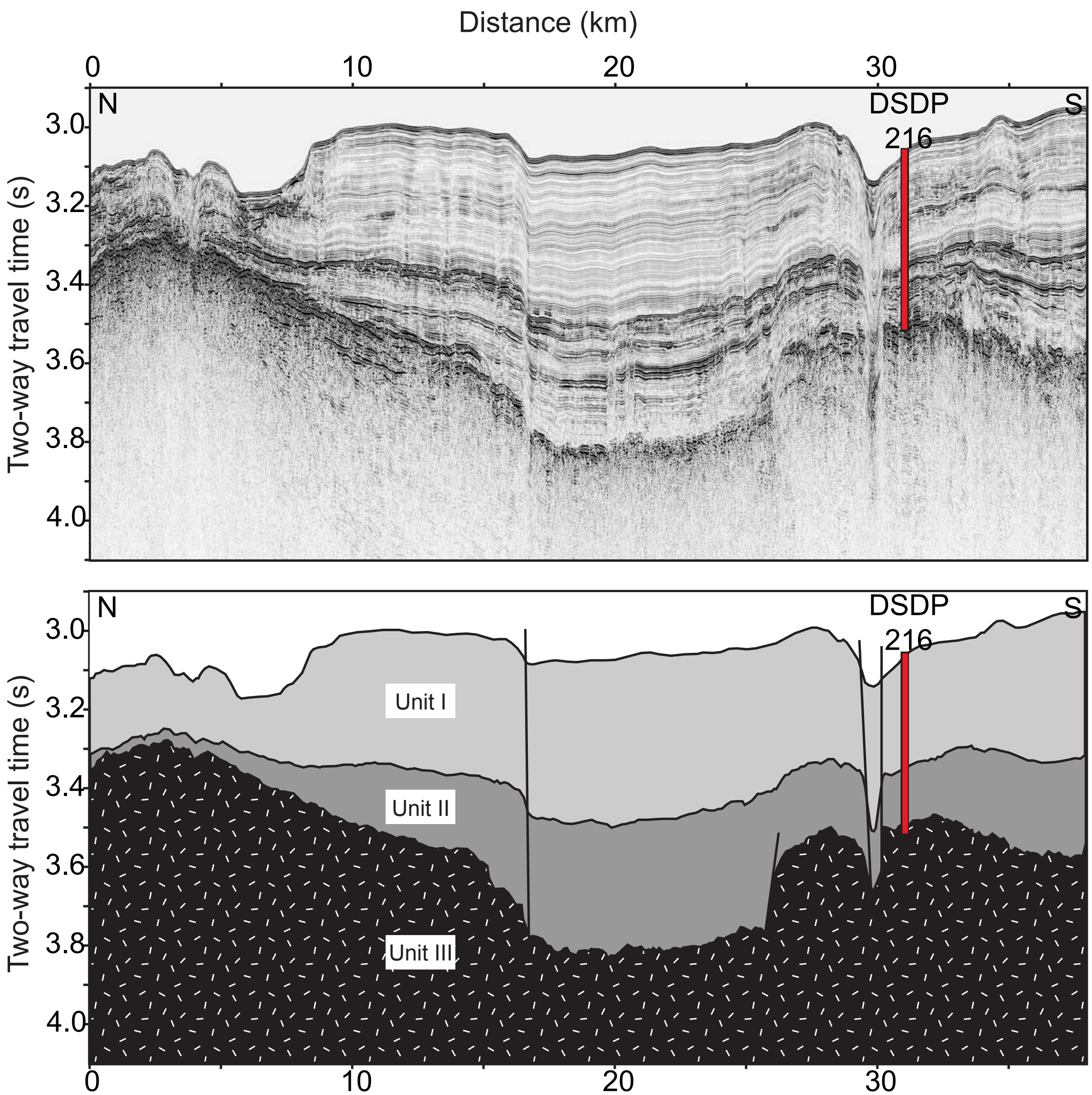

Figure 7. Seismic Reflection Profile from KNOX06RR Site 216. Conventions as in Figure 4.

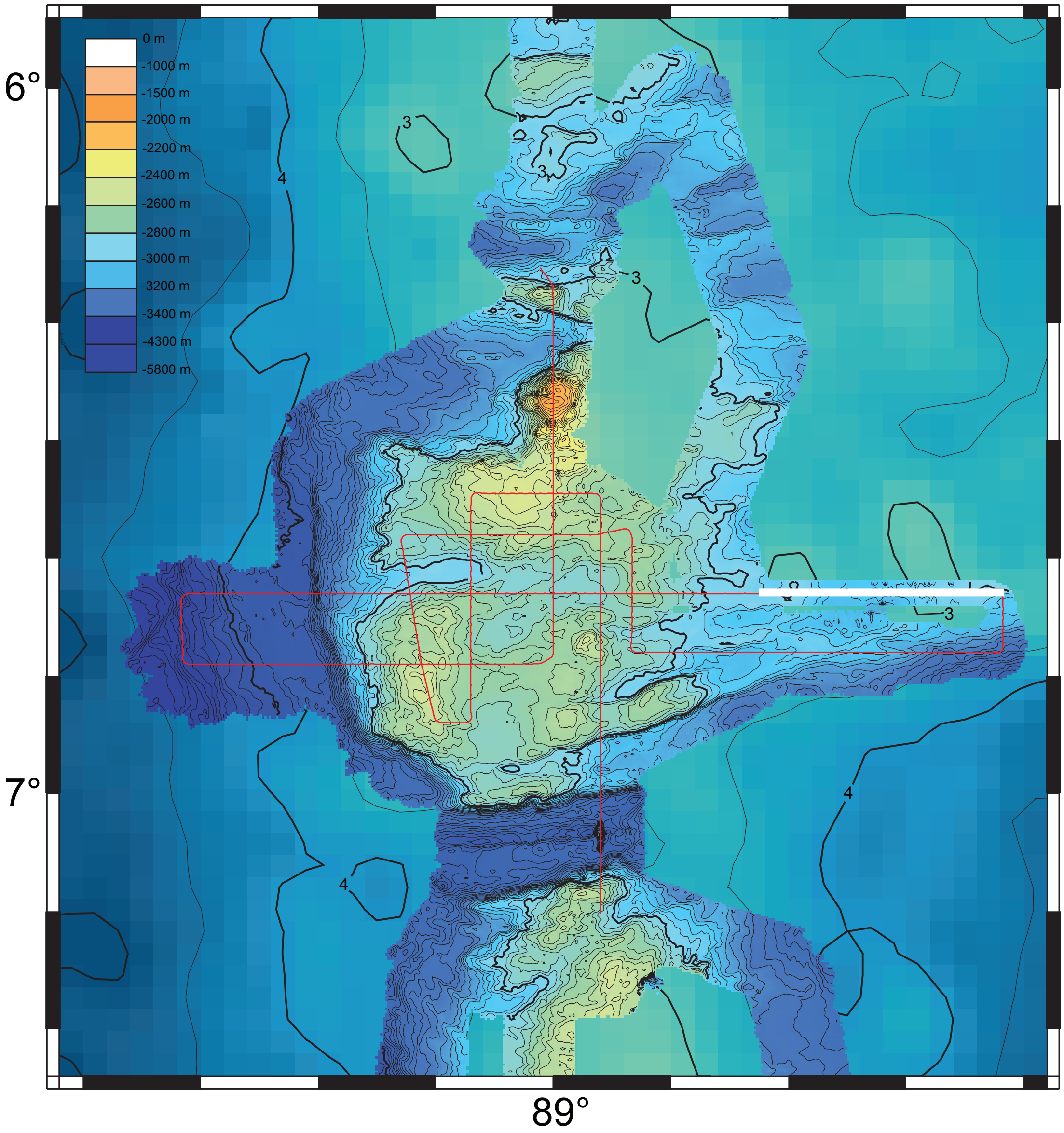

Figure 8. Seismic Survey Map of KNOX06RR Site NER2. Tracklines are shown in red. White bar indicates location of seismic profile in Figure 10. Conventions as in Figure 5.

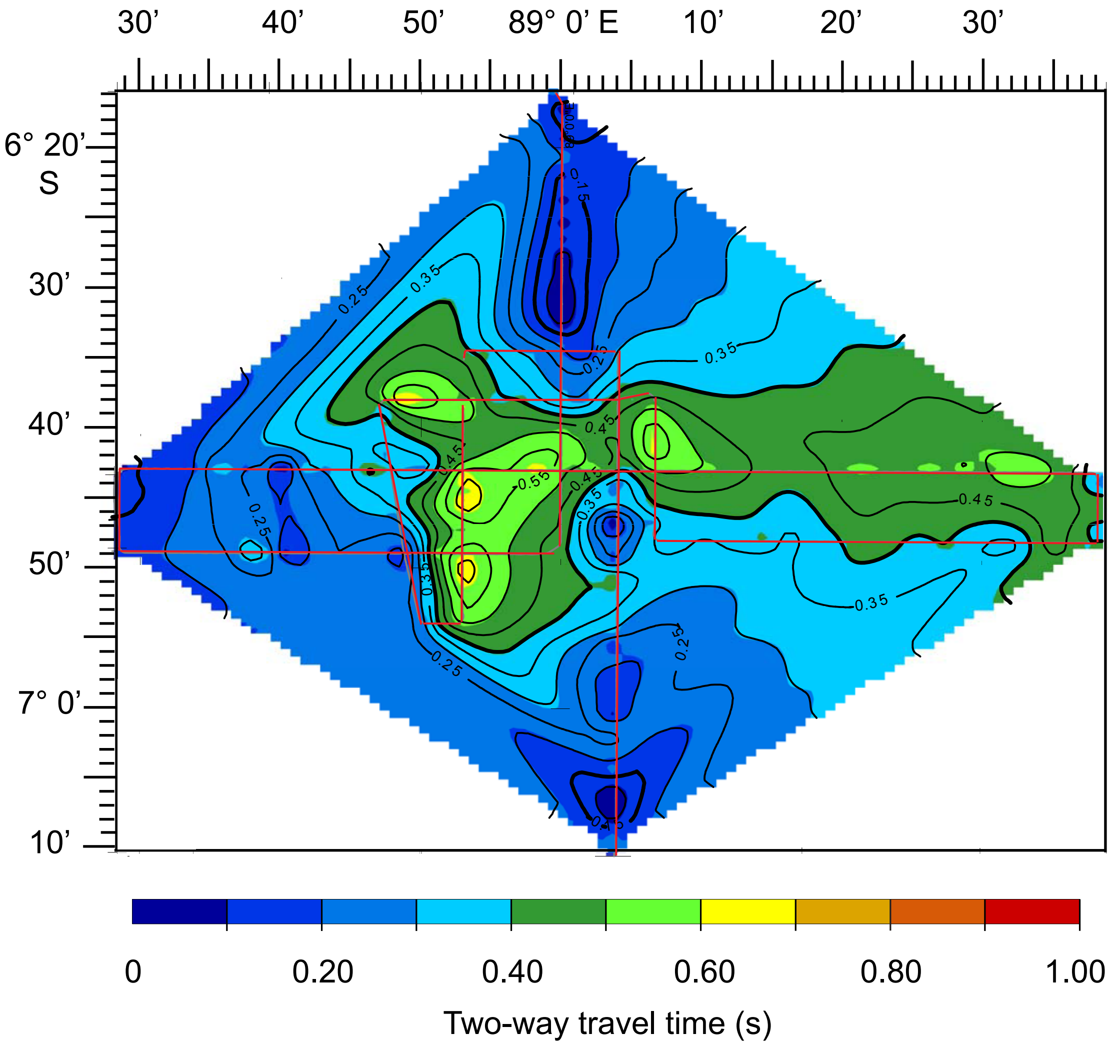

Figure 9. Total Sediment Thickness Isopach Map of KNOX06RR Site NER2. Conventions as in Figure 3.

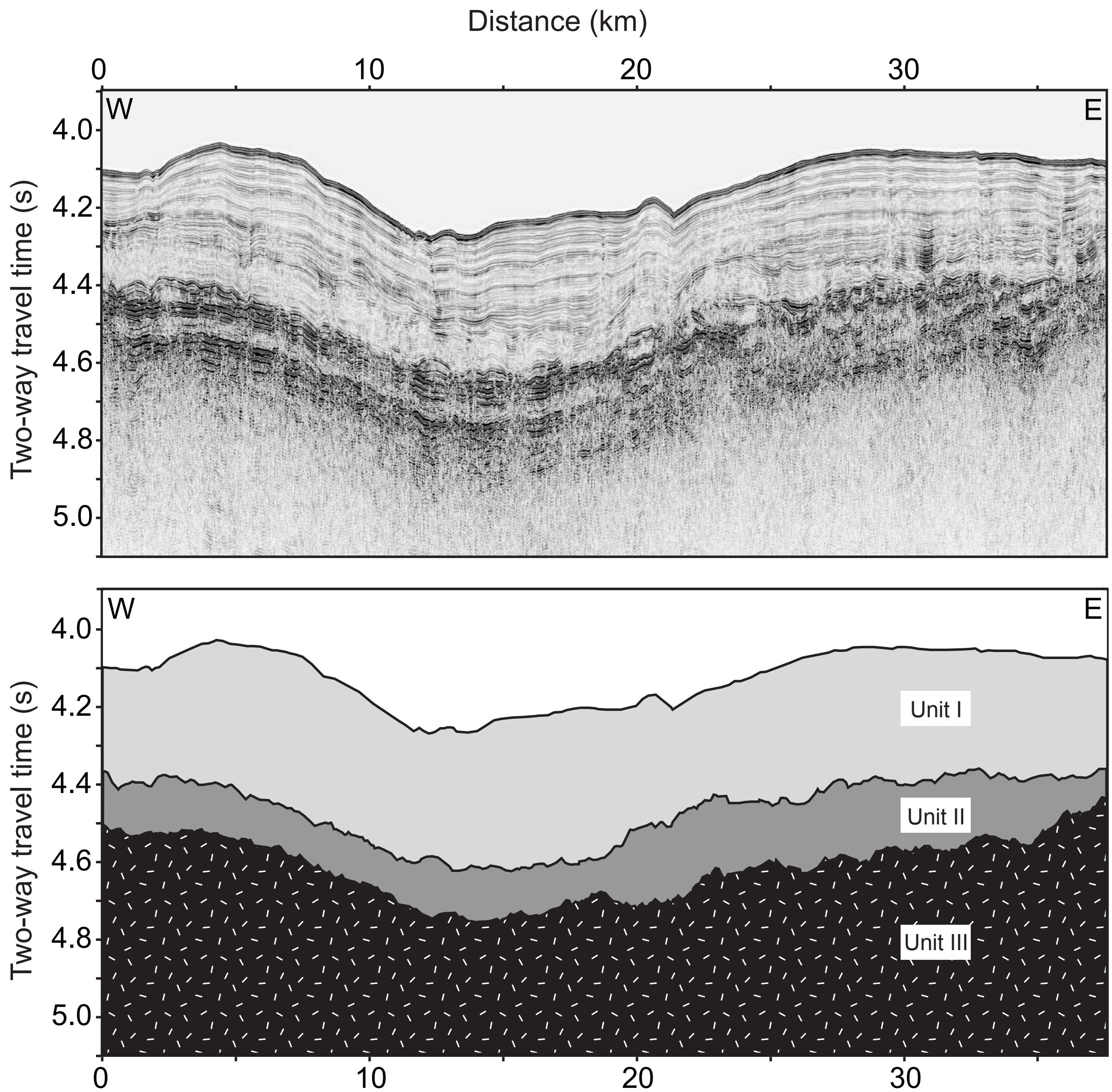

Figure 10. Seismic Reflection Profile from KNOX06RR Site NER2. Conventions as in Figure 4.

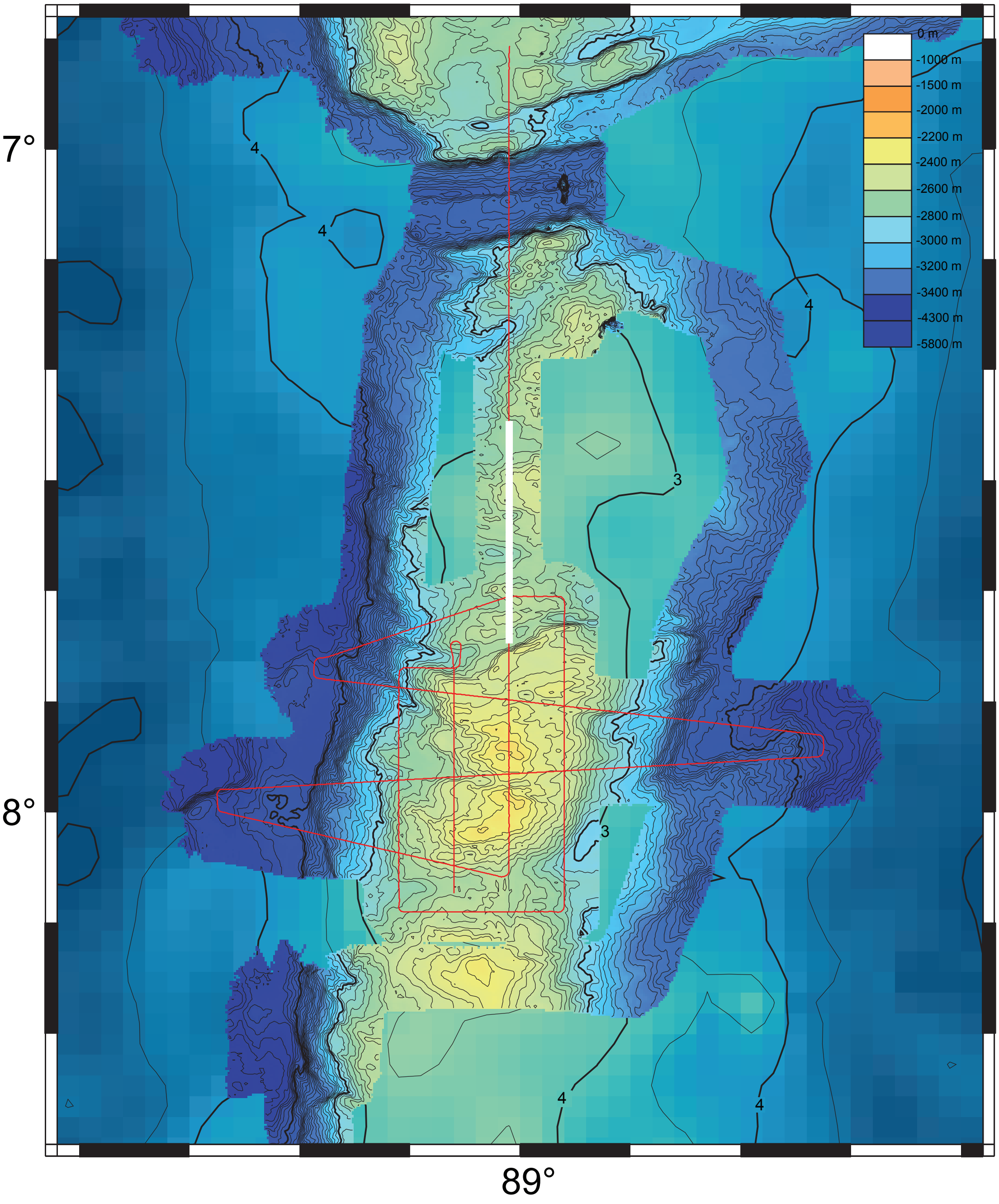

Figure 11. Seismic Survey Map of KNOX06RR Site NER3. Tracklines are shown in red. White bar indicates location of seismic profile in Figure 13. Conventions as in Figure 5.

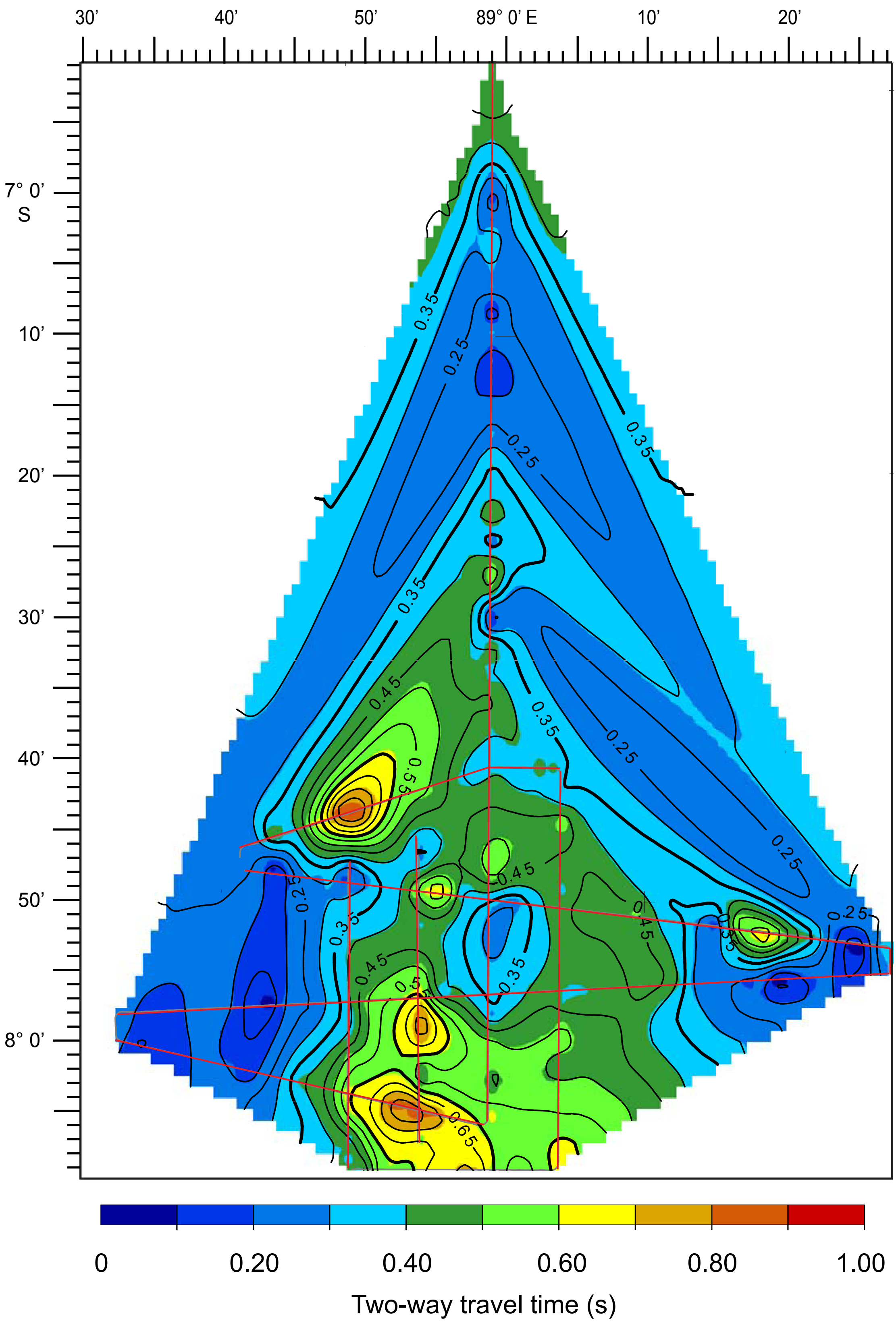

Figure 12. Total Sediment Thickness Isopach Map of KNOX06RR Site NER3. Conventions as in Figure 3.

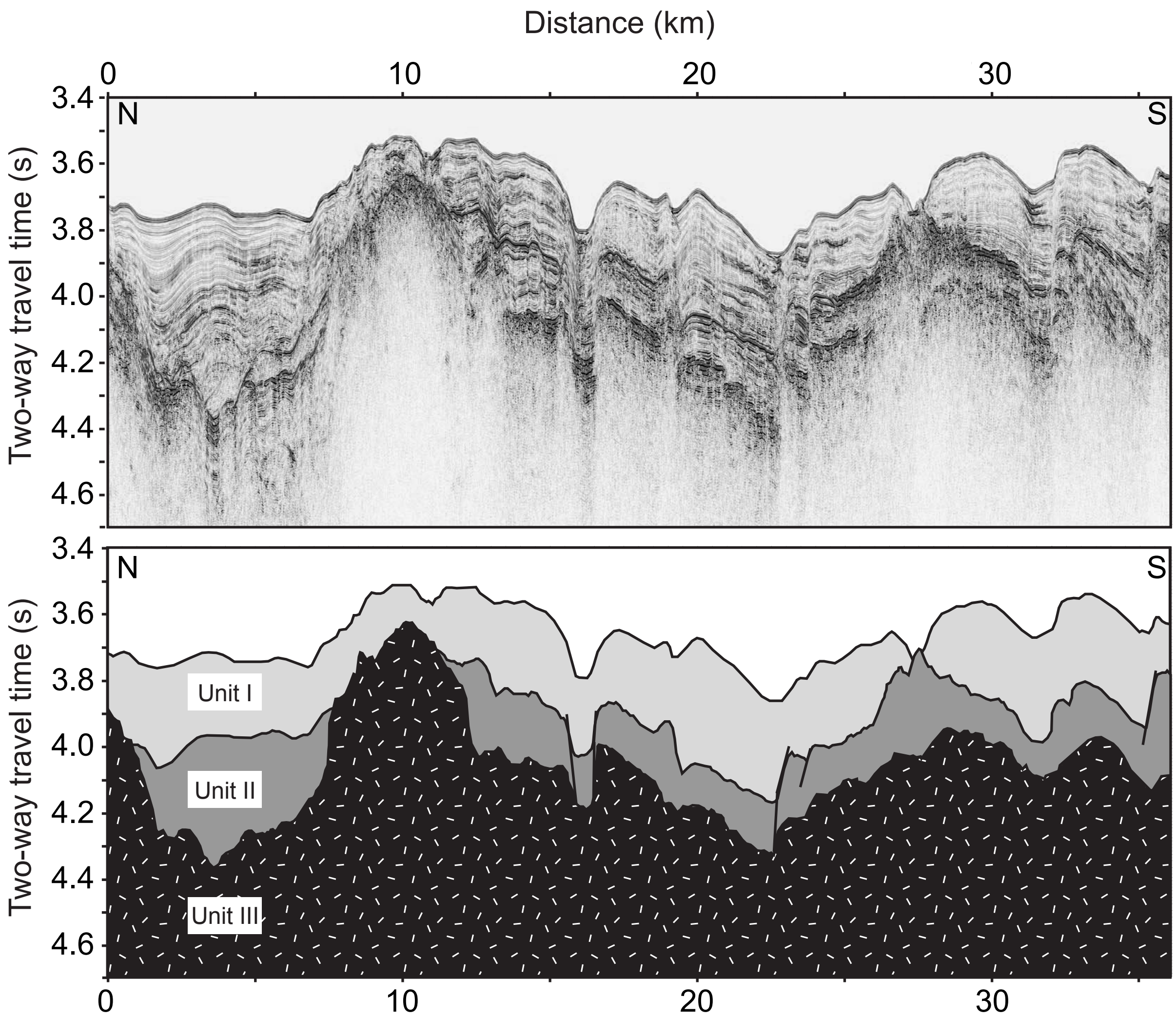

Figure 13. Seismic Reflection Profile from KNOX06RR Site NER3. Conventions as in Figure 4.

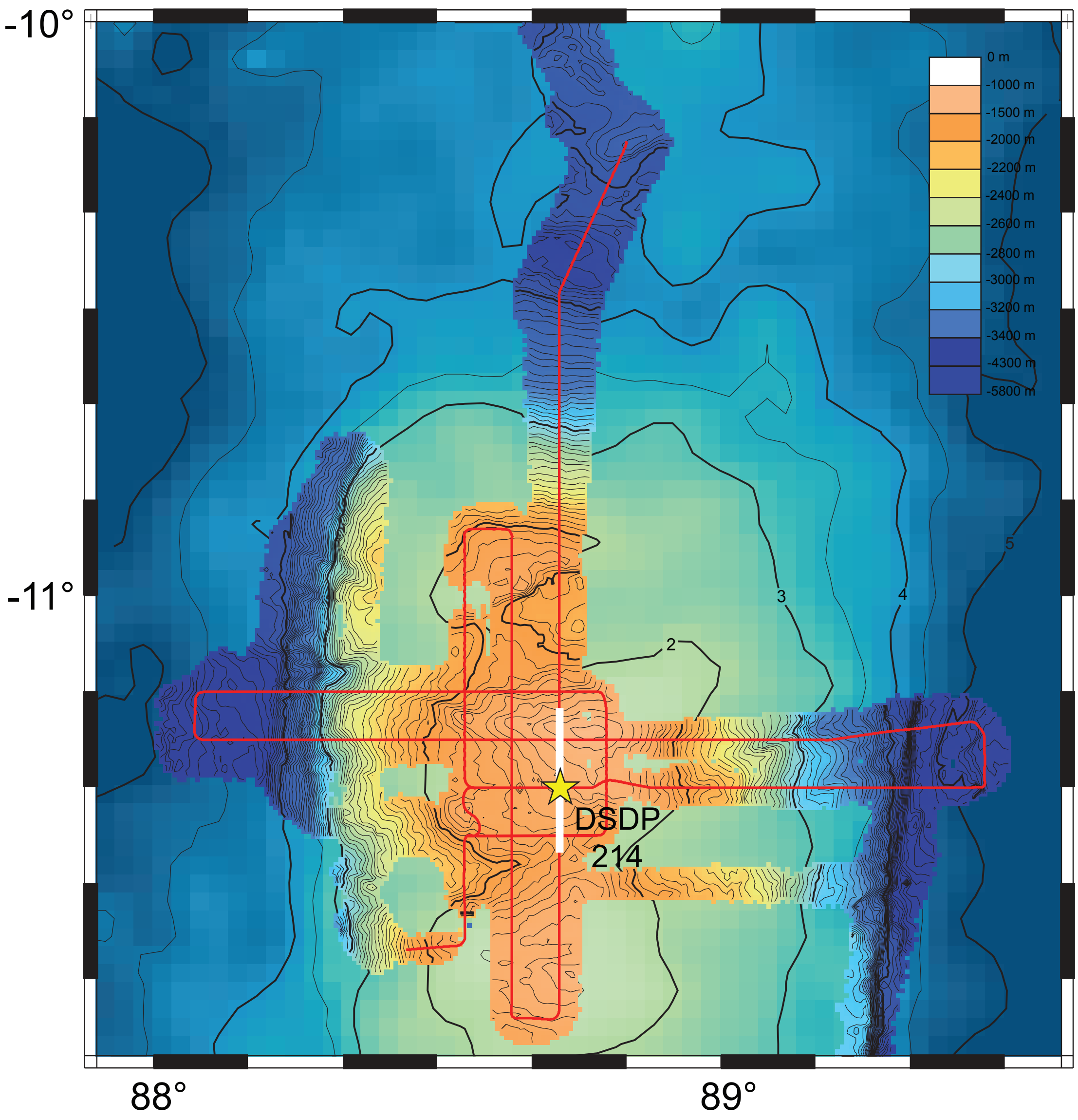

Figure 14. Seismic Survey Map of KNOX06RR Site 214. Tracklines are shown in red. White bar indicates location of seismic profile in Figure 16. Star indicates location of DSDP Site 214. Conventions as in Figure 5.

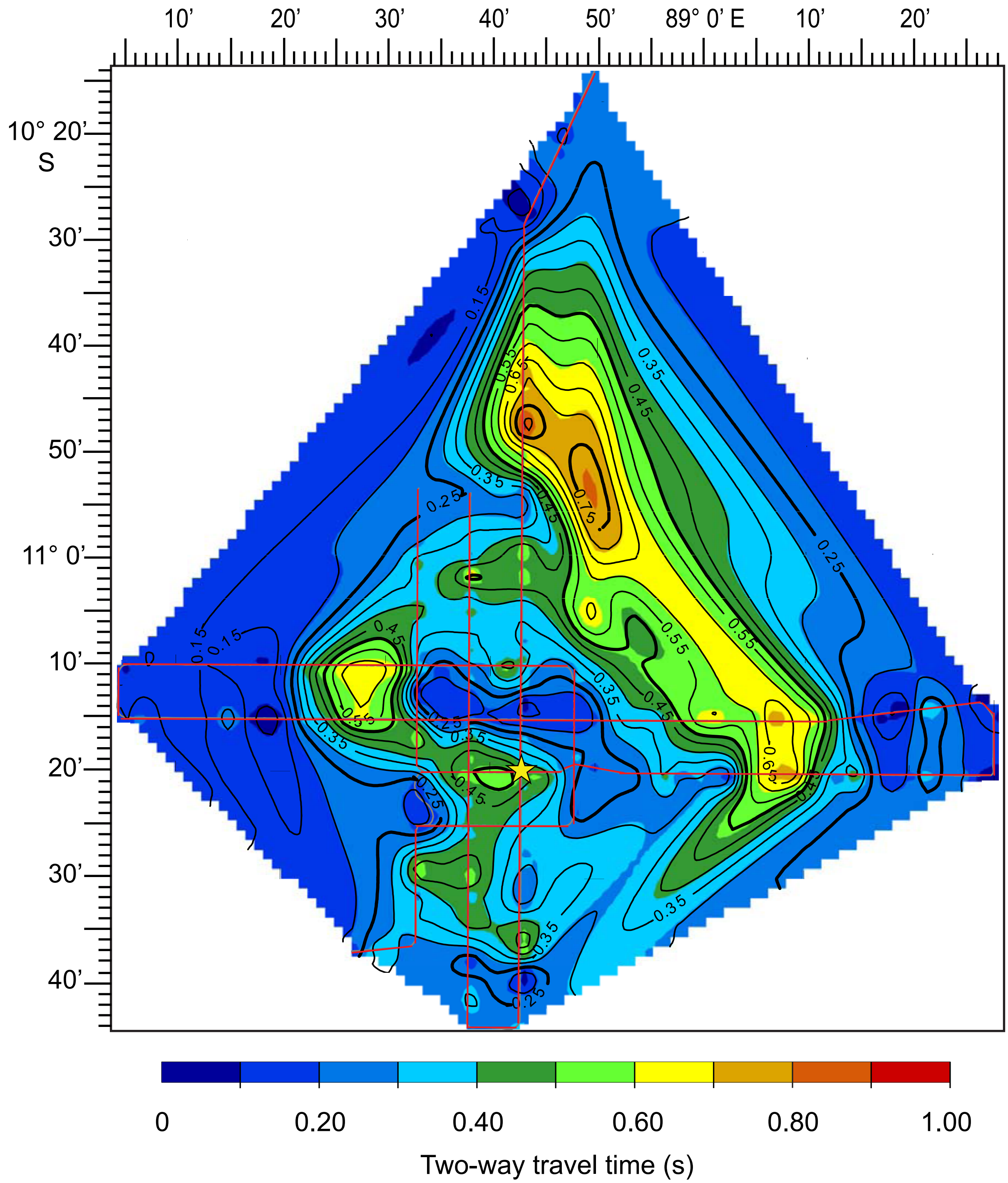

Figure 15. Total Sediment Thickness Isopach Map of KNOX06RR Site 214. Star indicates location of DSDP Site 214. Conventions as in Figure 3.

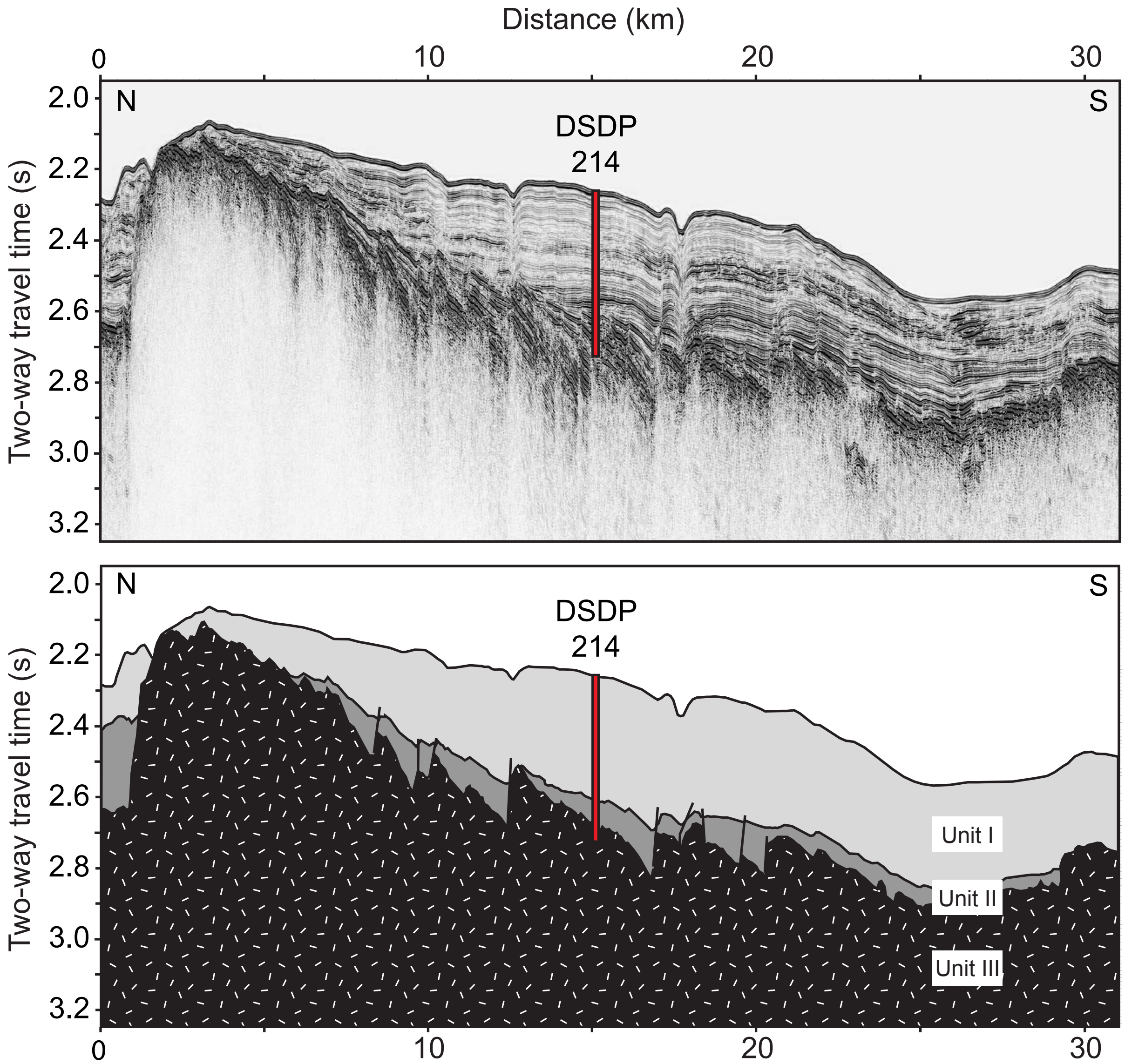

Figure 16. Seismic Reflection Profile from KNOX06RR Site 214. Conventions as in Figure 4.

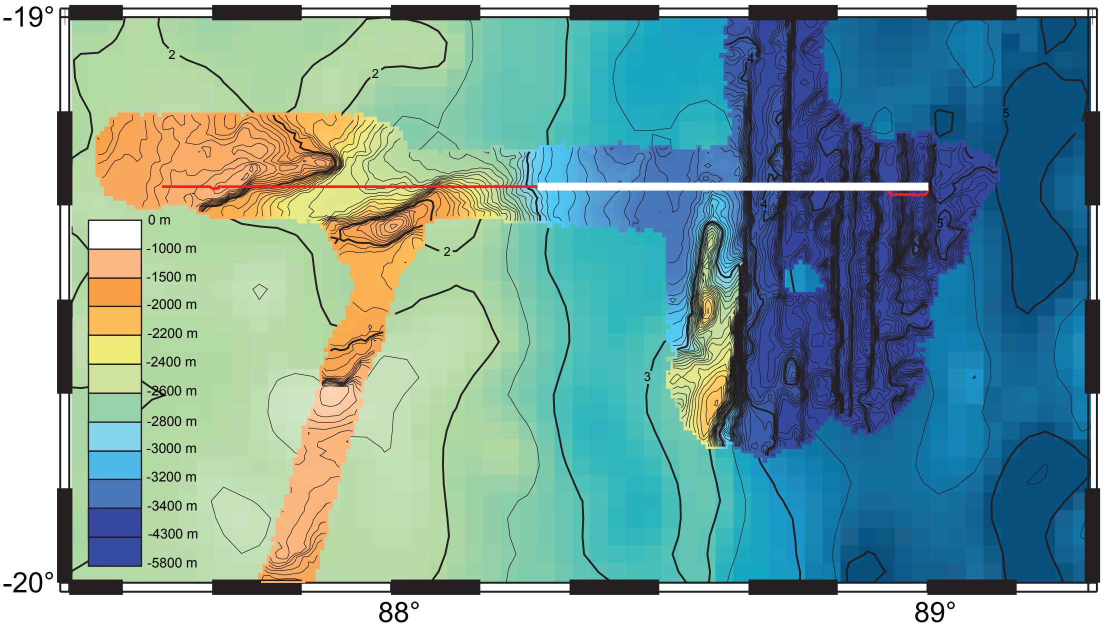

Figure 17. Seismic Survey Map of KNOX06RR Site NER4. Tracklines are shown in red. White bar indicates location of seismic profile in Figure 18. Conventions as in Figure 4.

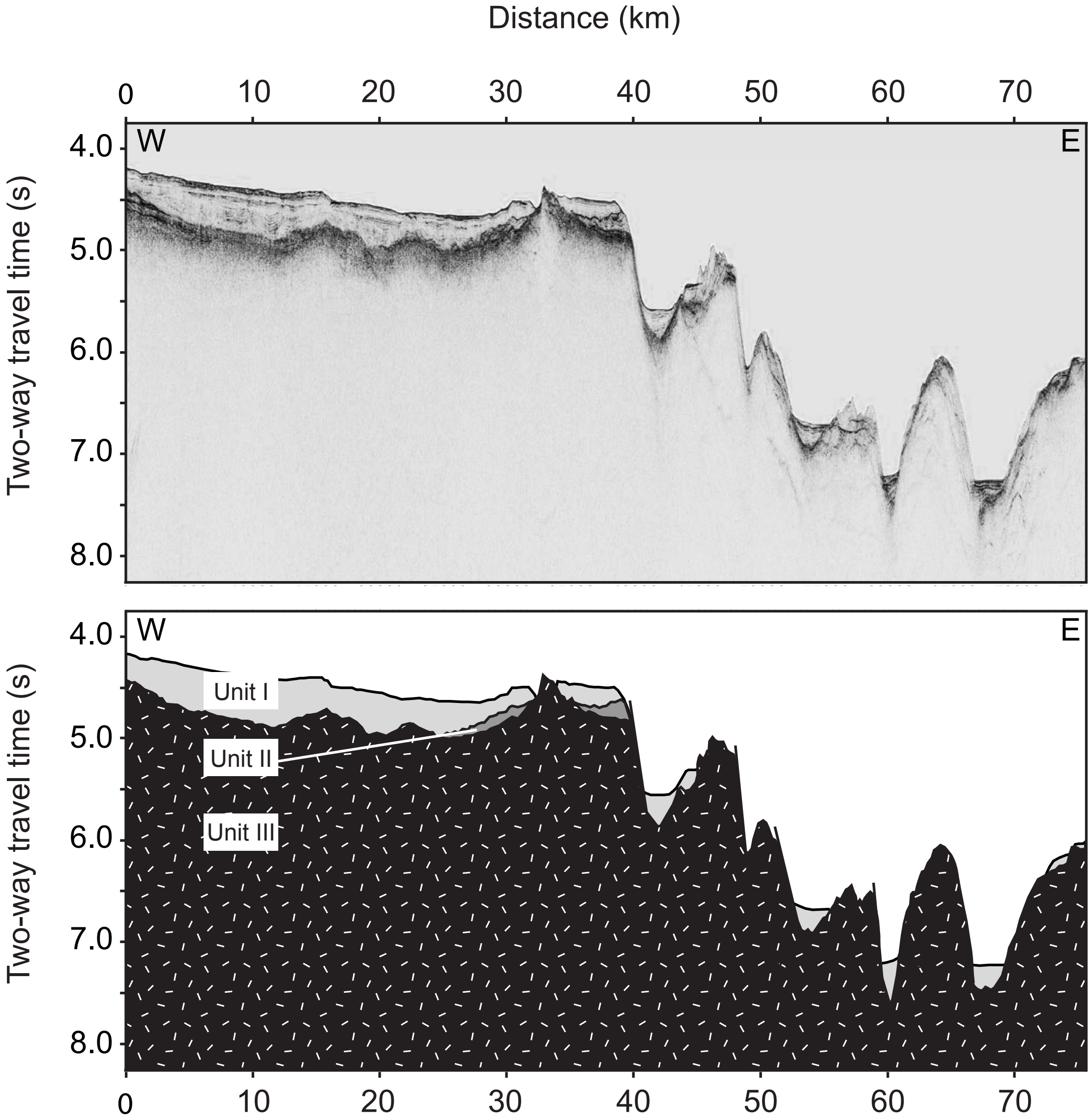

Figure 18. Seismic Reflection Profile from KNOX06RR Site NER4. Conventions as in Figure 4.

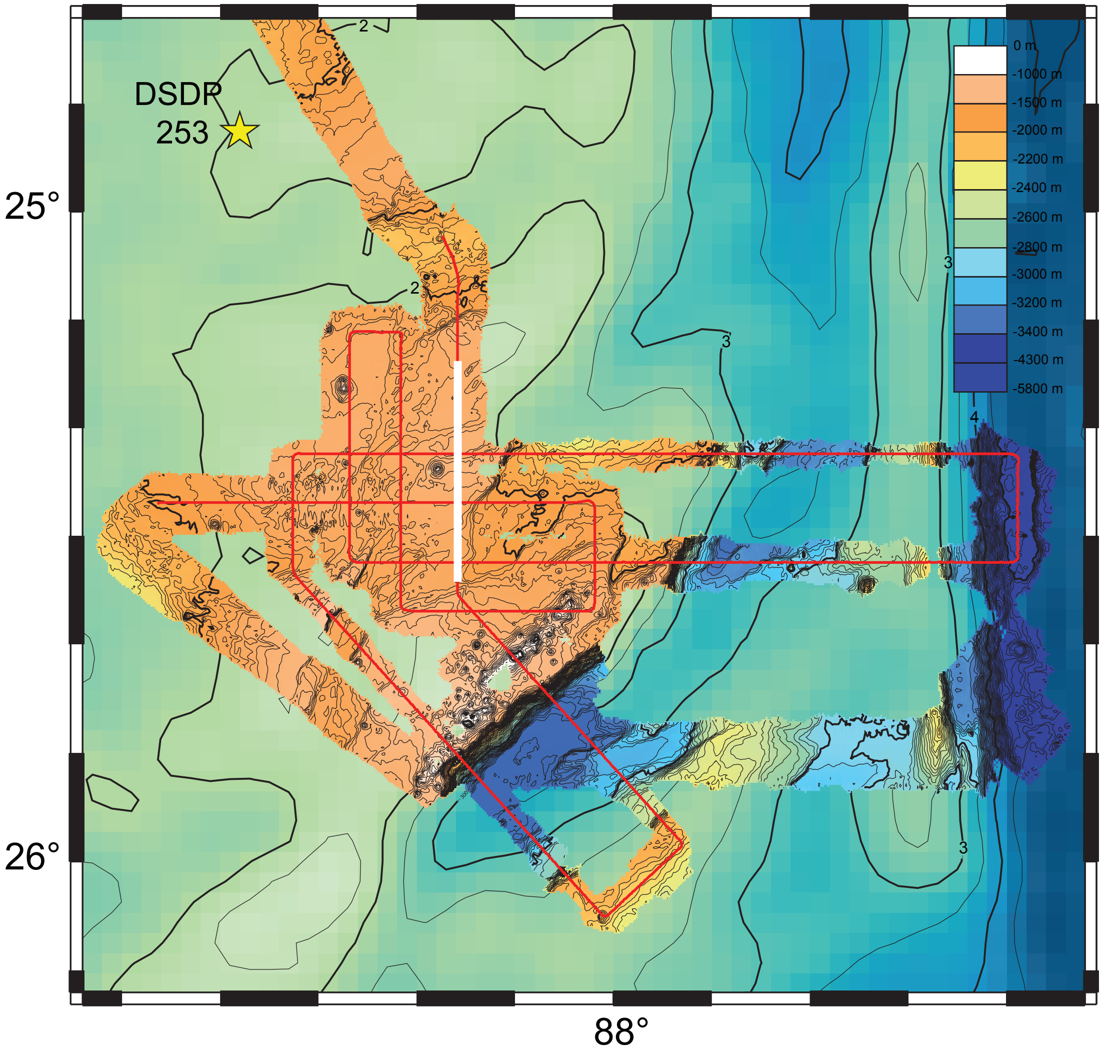

Figure 19. Seismic Survey Map of KNOX06RR Site 253. Tracklines are shown in red. White bar indicates location of seismic profile in Figure 21. Star indicates location of DSDP Site 253. Conventions as in Figure 5.

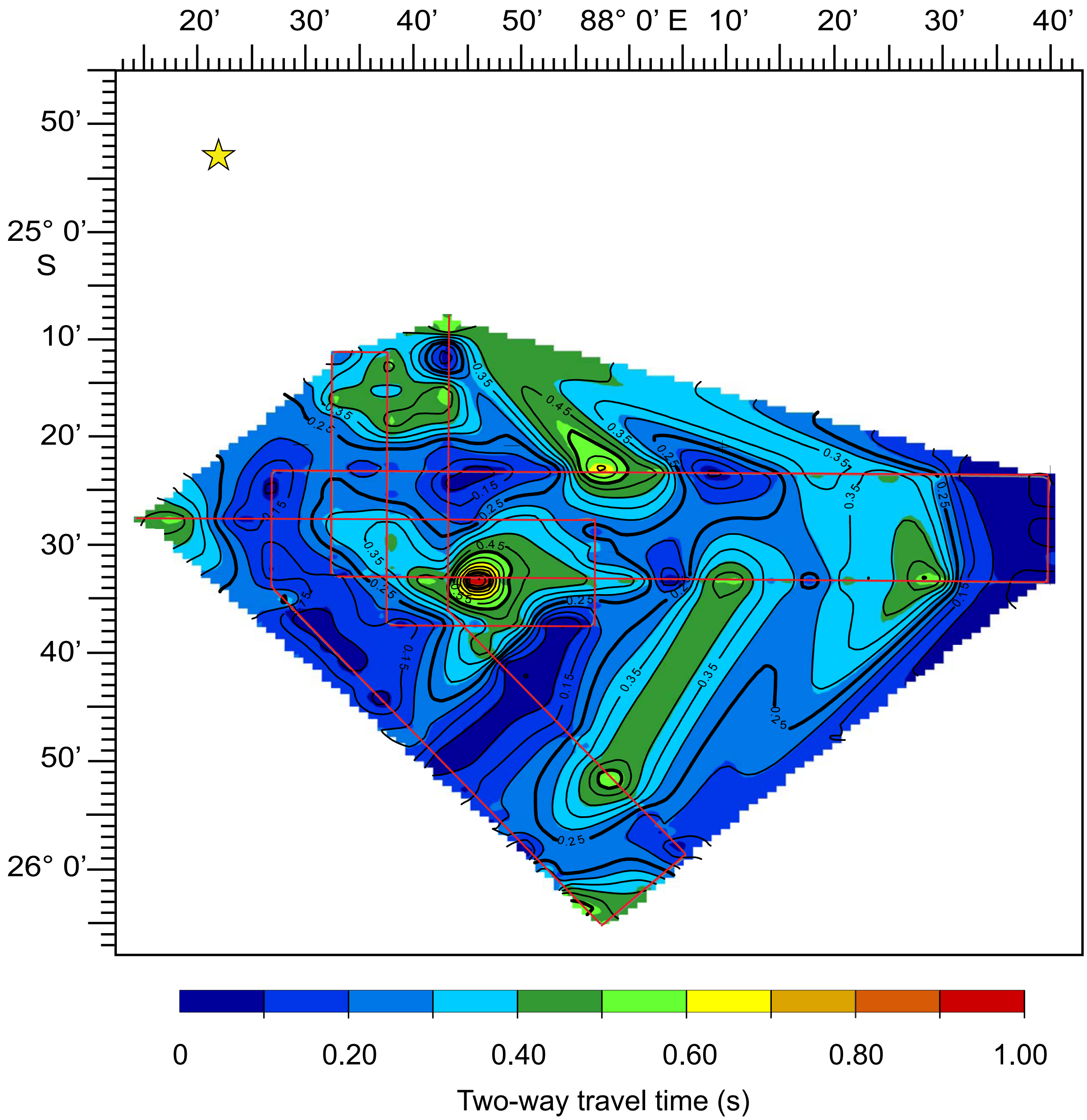

Figure 20. Total Sediment Thickness Isopach Map of KNOX06RR Site 253. Star indicates location of DSDP Site 253. Conventions as in Figure 3.

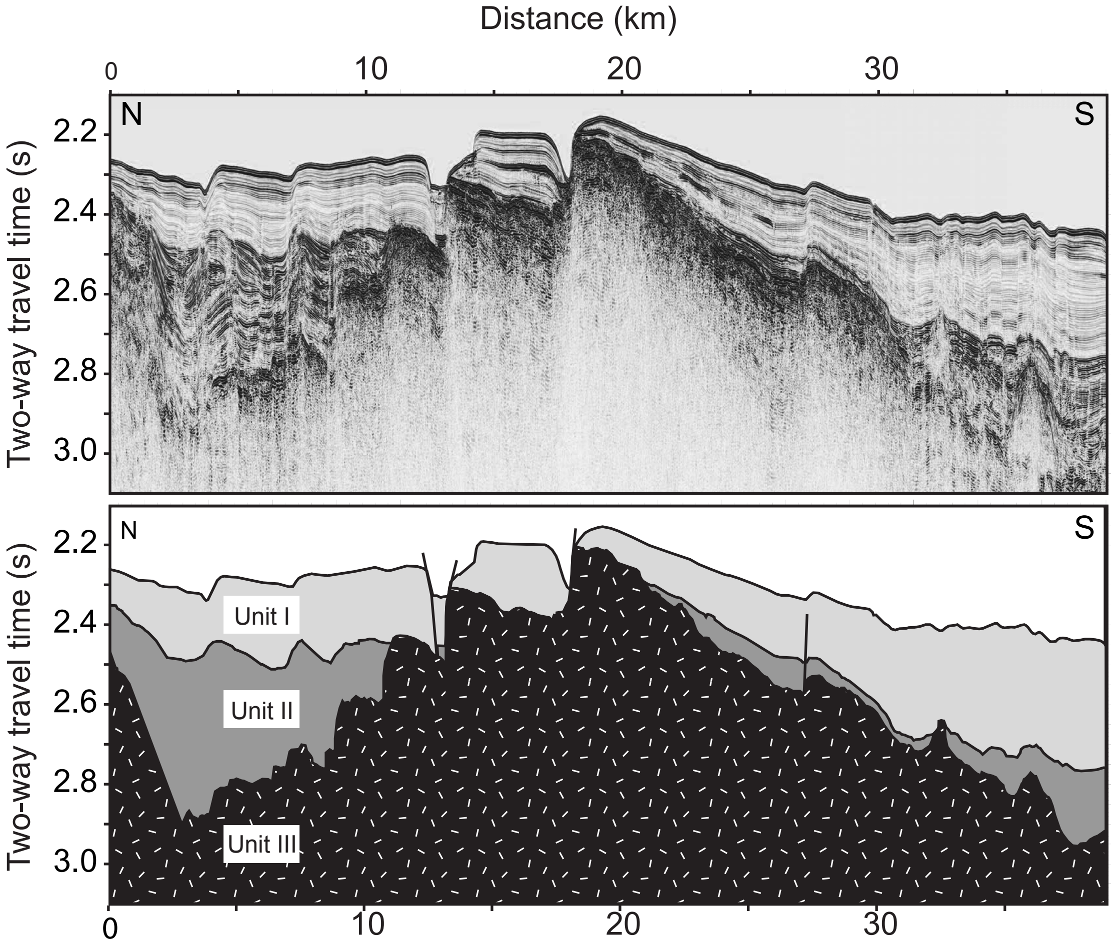

Figure 21. Seismic Reflection Profile from KNOX06RR Site 253. Conventions as in Figure 4.

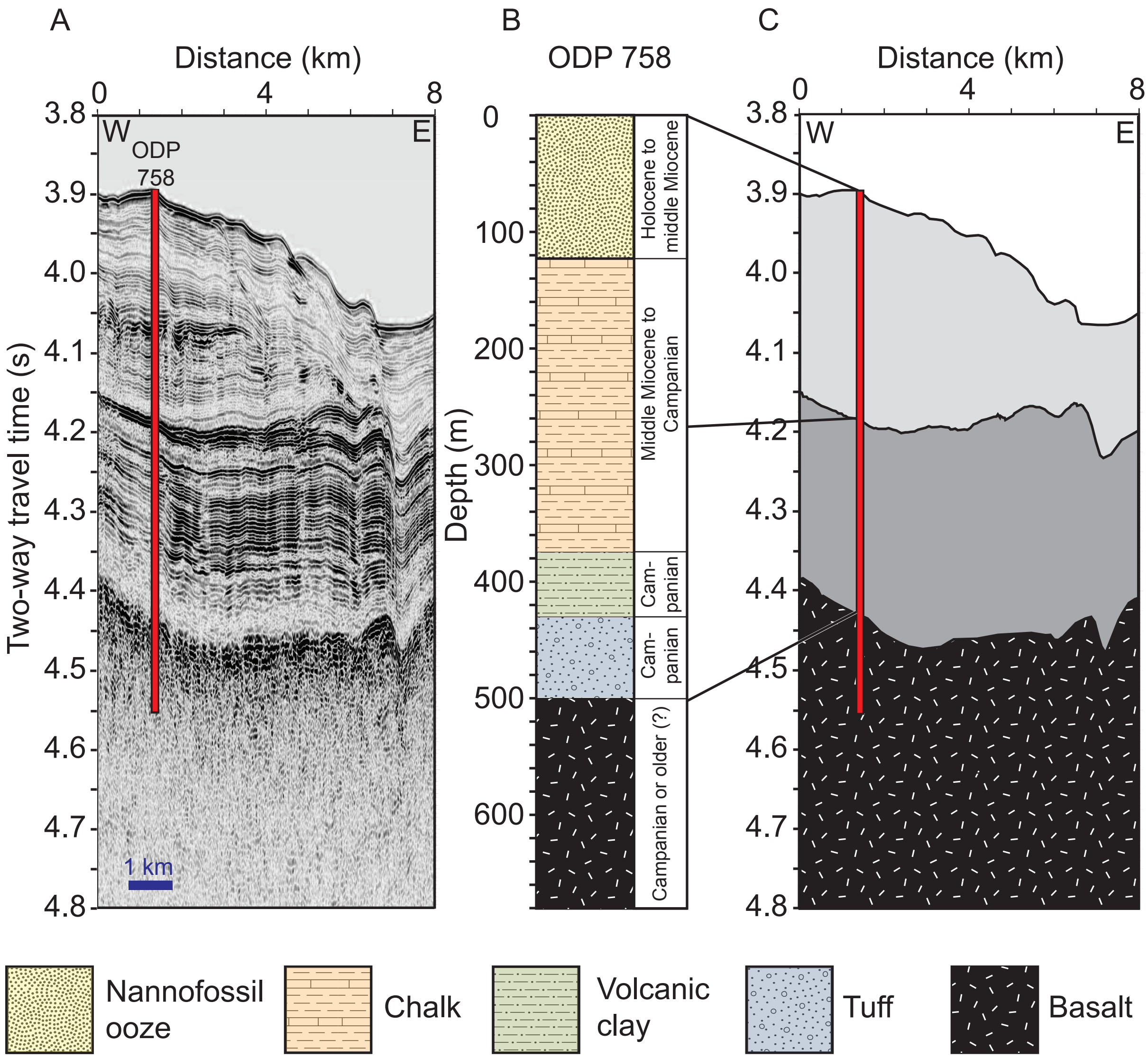

Figure 22. Correlation of Seismic Stratigraphy with ODP Site 758 Lithostratigraphy. a) KNOX06RR seismic reflection profile at ODP Site 758. Vertical red bar indicates approximate location and depth of drill hole. b) Stratigraphic column based on drilling results showing major lithologic types (Peirce, et al., 1989) with seismic stratigraphic correlation showing location of major horizons. c) Interpretation of seismic reflection profile showing three major seismic units shaded. Conversion from two-way travel time in seconds (s) to depth in meters (m) was made using ODP interval velocities (Peirce, et al., 1989).

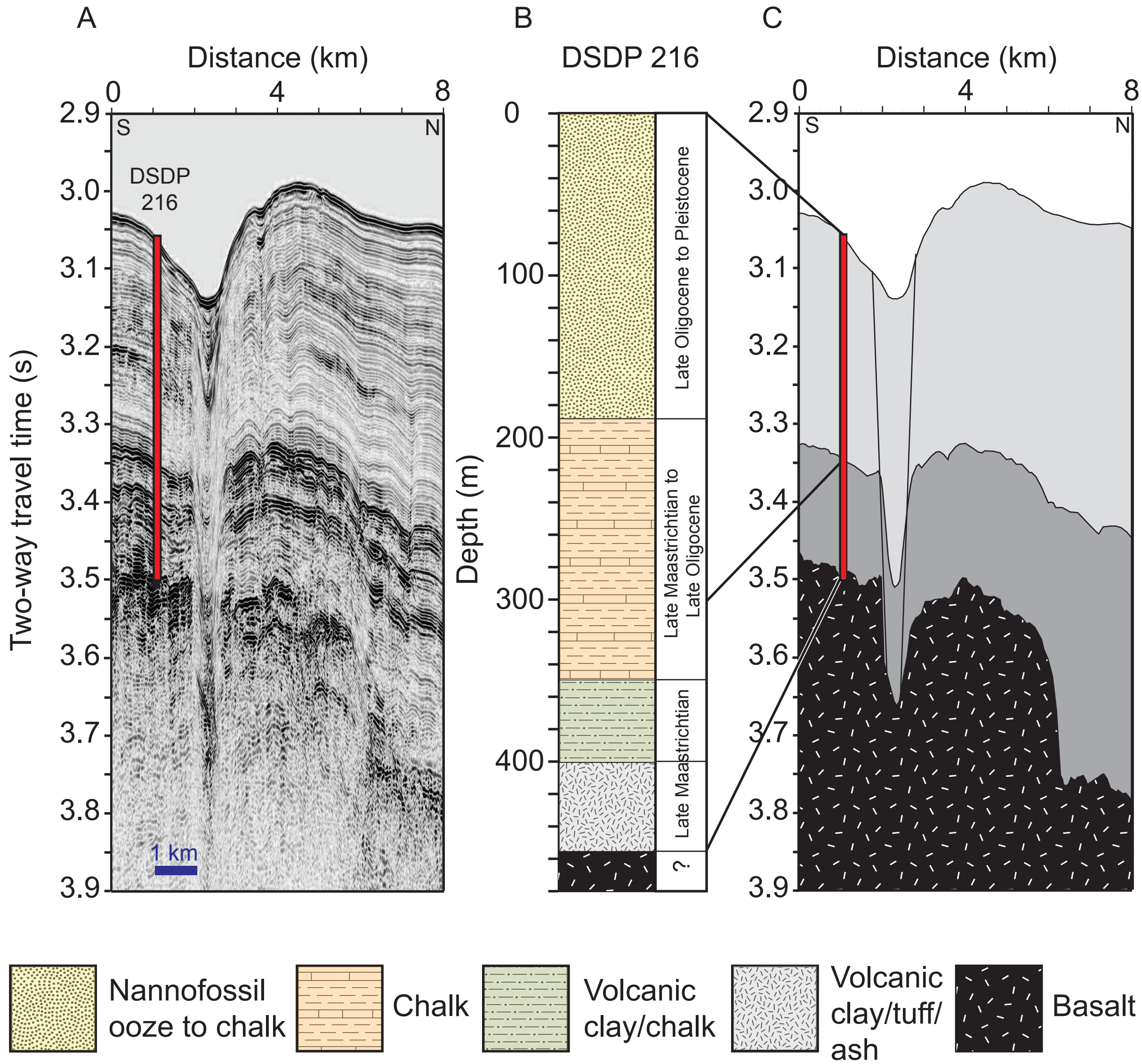

Figure 23. Correlation of Seismic Stratigraphy with DSDP Site 216 Lithostratigraphy. Conventions as in Figure 22. (von der Borch, et al., 1974)

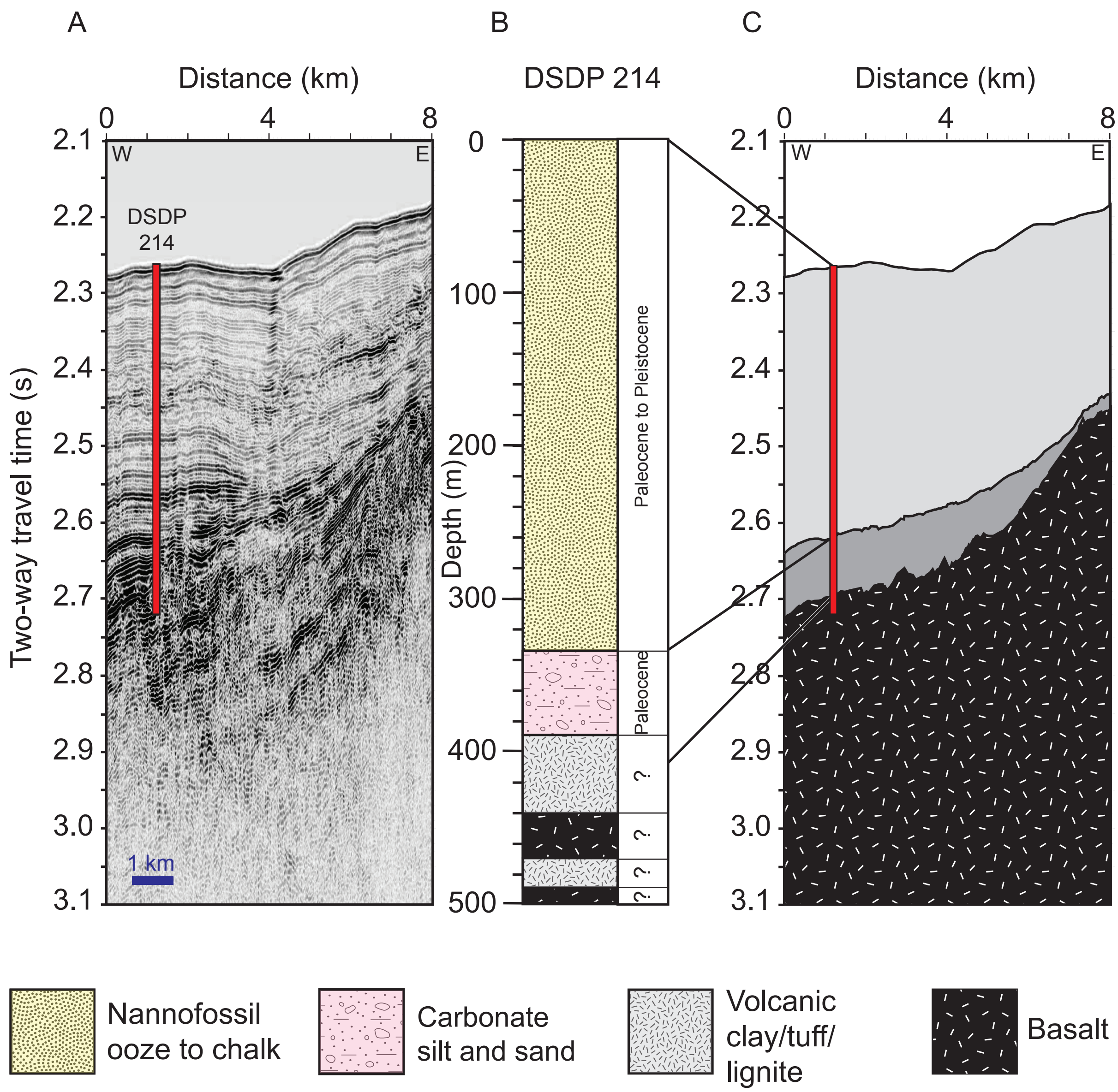

Figure 24. Correlation of Seismic Stratigraphy with DSDP Site 214 Lithostratigraphy. Conventions as in Figure 22. (von der Borch, et al., 1974)

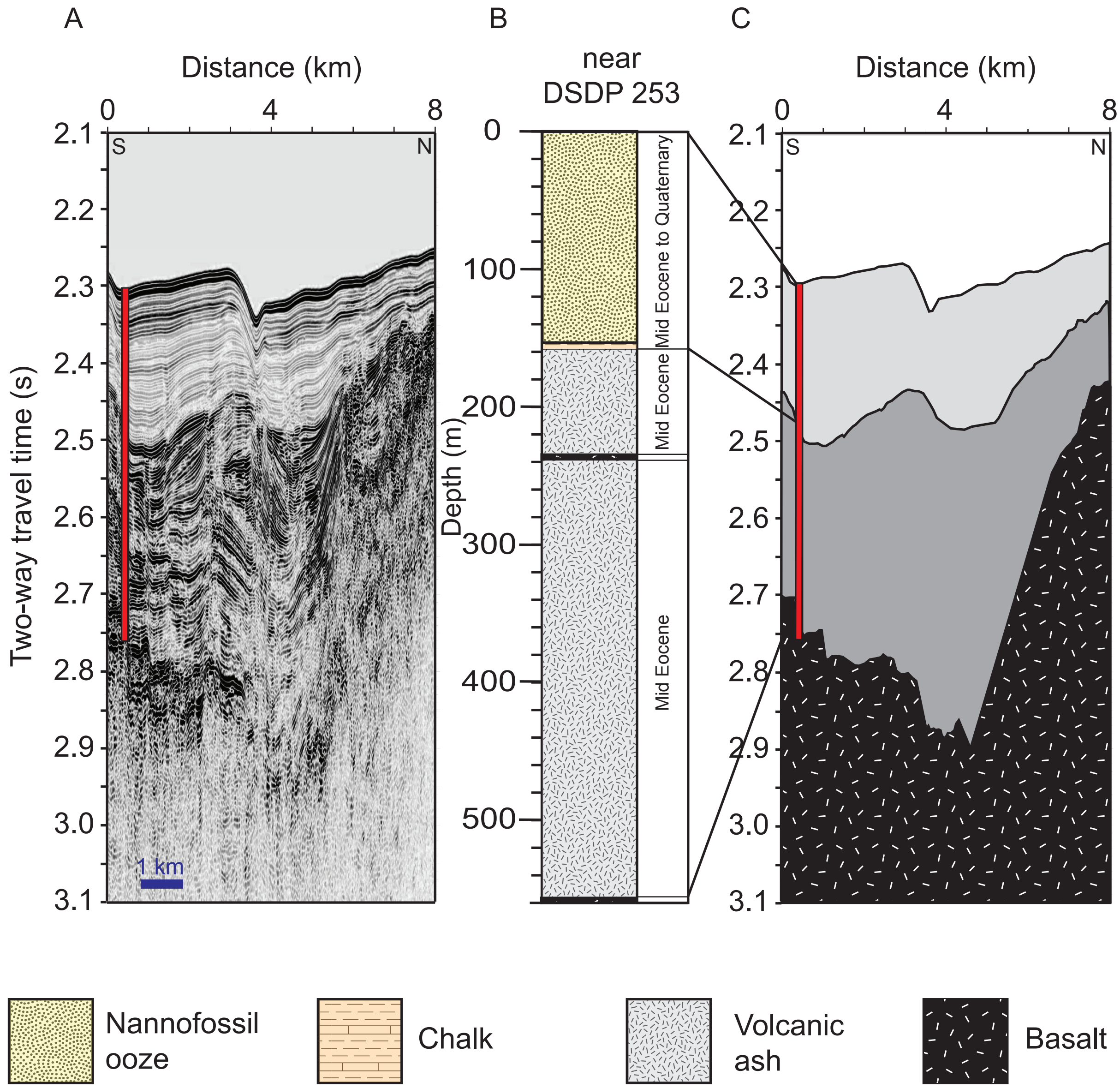

Figure 25. Correlation of Seismic Stratigraphy with DSDP Site 253 Lithostratigraphy. Note that this correlation is not made across DSDP Site 253 drillhole, but in the vicinity (~60 km) of the drill hole. Vertical red bar here represents approximate location and depth of drill hole as a reference. Conventions as in Figure 22. (Davies, et al., 1974)

APPENDIX B

TABLES

Table 1. KNOX06RR Seismic Data Acquisition Specifications. Cruise KNOX06RR, R/V Roger Revelle, Scripps Institution of Oceanography.

Length of tow leader	65 m
Length of tow stretch	25 m
Antenna to stern	40 m
Antenna height	25 m
Center of near trace	136.25 m
Center of far trace	723.75 m
Gun setback from antenna	64 m
Near inline offset	72.25 m
Active cable	600 m
Far inline offset	659.75 m
Gun setback from stern	24 m
Source type	2 GI guns (45 in^3/105 in^3)
Source depth	4 m
Pre-amp gain	24 dB
Cable depth	3-5 m
No. channels	48
Digital recording system	GeoEel
SEG format	D 8058 Rev 1
Record length	9 s
Sample interval	500 ms
Near offset	136.25 m
Far offset	723.75 m
Near trace no.	1
Far trace no.	48
Group interval	12.5 m
Shooting interval	10s @ 6 knots

VITA

Name: Amy Elizabeth Eisin

Address: In care of the Department of Oceanography
Texas A&M University
Eller O&M Building
MS 3146
College Station, TX 77843-3146

Education: B.S., Geology, University of Illinois at Urbana-Champaign, 2003
M.S., Oceanography, Texas A&M University, College Station, 2009

Publications and Presentations:

Eisin, A. E.; Sager, W. W. (2008), Seismic Stratigraphy of Ninetyeast Ridge Sediments. American Geophysical Union Fall Meeting, abstract #T51B-1893 and poster presentation

Paul, C. F.; Sager, W. W.; Pringle, M. S.; **Eisin**, A. E. (2008), Tectonic Fabric of the Ninetyeast Ridge, Central Indian Ocean: Implications for Ridge Formation. American Geophysical Union Fall Meeting, abstract #T51B-1874

Levchenko, O.; **Eisin, A. E.**; Ivanenko, A. N.; Marinova, J. G.; Paul, C. F.; Sborshchikov, I. M.; Sager, W. W. (2008), Detailed structure and tectonics of the Ninetyeast Ridge near Site ODP 758 (on new geophysical data from KNOX06RR cruise of R/V *Roger Revelle*). American Geophysical Union Fall Meeting, abstract #T51B-1875

Eisin, A. E., et al. (2007), Preliminary Geophysical Results from the Ninetyeast Ridge Expedition, American Geophysical Union Fall Meeting, abstract #V21B-0610 and poster presentation